

## Accepted Manuscript

A concise review of nanoscopic aspects of bioleaching bacteria-mineral interactions

Mengxue Diao, Elena Taran, Stephen Mahler, Anh Nguyen

PII: S0001-8686(14)00247-4  
DOI: doi: [10.1016/j.cis.2014.08.005](https://doi.org/10.1016/j.cis.2014.08.005)  
Reference: CIS 1474

To appear in: *Advances in Colloid and Interface Science*



Please cite this article as: Diao Mengxue, Taran Elena, Mahler Stephen, Nguyen Anh, A concise review of nanoscopic aspects of bioleaching bacteria-mineral interactions, *Advances in Colloid and Interface Science* (2014), doi: [10.1016/j.cis.2014.08.005](https://doi.org/10.1016/j.cis.2014.08.005)

This is a PDF file of an unedited manuscript that has been accepted for publication. As a service to our customers we are providing this early version of the manuscript. The manuscript will undergo copyediting, typesetting, and review of the resulting proof before it is published in its final form. Please note that during the production process errors may be discovered which could affect the content, and all legal disclaimers that apply to the journal pertain.

**A concise review of nanoscopic aspects of bioleaching bacteria-mineral interactions**

Mengxue Diao<sup>1</sup>, Elena Taran<sup>2</sup>, Stephen Mahler<sup>1,2</sup>, Anh Nguyen<sup>1\*</sup>

<sup>1</sup>School of Chemical Engineering

The University of Queensland, St Lucia, 4072, Queensland, Australia

<sup>2</sup>Australian Institute for Bioengineering and Nanotechnology, ANFF-Q

The University of Queensland, Brisbane, QLD 4072, Australia

\*Corresponding Author: Phone +61-7-33653665, Email: anh.nguyen@eng.uq.edu.au

**Abstract**

Bioleaching is a technology for the recovery of metals from minerals by means of microorganisms, which accelerate the oxidative dissolution of the mineral by regenerating ferric ions. Bioleaching processes take place at the interface of bacteria, sulfide mineral and leaching solution. The fundamental forces between a bioleaching bacterium and mineral surface are central to understanding the intricacies of interfacial phenomena, such as bacterial adhesion or detachment from minerals and the mineral dissolution. This review focuses on the current state of knowledge in the colloidal aspect of bacteria-mineral interactions, particularly for bioleaching bacteria. Special consideration is given to the microscopic structure of bacterial cells and the atomic force microscopy technique used in the quantification of fundamental interaction forces at nanoscale.

**Keywords:** Bioleaching, bacterial adhesion, atomic force microscopy, interaction forces

**Contents**

Abstract.....	1
1. Introduction .....	2
2. Bioleaching and metal sulfide oxidizing microorganisms .....	3
2.1 Bioleaching.....	3
2.2 Diversity of bioleaching microorganisms .....	4
2.3 Microscopic structures of bioleaching bacteria.....	8

2.3.1	Cell wall.....	8
2.3.2	Surface appendages.....	10
2.3.3	Extracellular polymeric substances (EPS).....	11
2.4	Macroscopic cell surface properties.....	13
2.5	Bacterial adhesion mechanism in the interfacial process of bioleaching.....	15
3.	Applications of AFM in bacterial adhesion research.....	17
3.1	Principles of AFM.....	18
3.2	Immobilization of bacterial cells.....	20
3.3	Applications of AFM in bioleaching research.....	23
3.3.1	AFM imaging.....	23
3.3.2	AFM force measurements.....	27
3.3.3	Nanomechanical properties.....	32
4.	Theories for the interacting forces.....	34
4.1	Classical DLVO theory.....	34
4.2	Extended DLVO theory.....	40
4.3	Thermodynamic approach.....	41
4.4	Steric model.....	42
5.	Concluding remarks.....	44
	Acknowledgements.....	44
	References.....	45

## 1. Introduction

Bioleaching is the process of extracting metals from sulfides and/or iron-containing ores using microbiological technology. The majority of the leaching bacteria in a bioleaching system live in communities that attach on the surface of mineral sulfides [1]. The adhesion of bacterial cells on mineral surfaces has been recognized for decades, and it is essentially one of the most important aspects determining the success of bioleaching processes [2]. Therefore, fundamental understanding of bioleaching processes requires information on the interaction of the bacteria and the solid mineral surfaces.

Bacterial adhesion is generally controlled by both long-range interactions and adhesion forces between bacterial cell and mineral surfaces. The fundamental forces between a bacterium and mineral surface are central to understanding the intricacies of interfacial phenomena, especially in the non-contact bioleaching mechanism. Non-specific interaction forces governing the initial phase of the bacterial adhesion basically include the attractive Lifshitz

van der Waals interaction and the electrostatic double layer interaction, which have been well described in the classical Derjaguin-Landau-Verwey-Overbeek (DLVO) theory of colloid stability.

The DLVO theory has been widely used to qualitatively and quantitatively calculate adhesion free energy involved in bacterial adhesion [3-5]. However, in many cases the classic DLVO theory cannot successfully explain the direct measured surface forces in a liquid medium because bacteria are living entities with complicated cell surface structures and appendages. Under these circumstances, an additional term called the short-range Lewis acid-base (AB) interaction is introduced into the extended DLVO theory [6]. Surface hydrophobicity and surface electric charge are of importance in bacterial adhesion. The contact angle measurements were used to calculate the balance of interfacial free energies between involved surfaces by the thermodynamic approach [7, 8].

Atomic force microscopy (AFM) is a powerful tool for providing high-resolution images as well as probing interaction forces in the biological area which was intensively reviewed [9, 10]. A variety of immobilization methods have been developed and compared to attach bacterial cells to solid surfaces for the AFM force measurement [11]. The interactions between bacteria and solid surfaces have been quantitatively studied and theoretically modelled [5, 12-16], but only a few were dealing with bioleaching.

This review mainly deals with the colloidal aspects of bacterial adhesion in bioleaching systems. Investigations are reviewed where the DLVO theory, steric model and AFM force measurements have been used to explain colloidal aspects of bacterial adhesion.

## **2. Bioleaching and metal sulfide oxidizing microorganisms**

### **2.1 Bioleaching**

Bioprocessing is a generic term that describes the processing of using (micro-) biological technology to extract metals from sulfide and/or iron-containing ores and mineral concentrates [17]. More precisely, it uses the catalytic effect produced by the metabolic activity of some iron-oxidizing and sulfur-oxidizing microorganisms resulting in an acceleration of the chemical degradation of the ores [18].

Bioprocessing was applied by the mineral industry prior to the understanding of the role of microorganisms in metals extraction. An early documented commercial application of a biohydrometallurgy process in the mining industry was for copper extraction from mine waste [19]. Until 1947, following the discovery that microorganisms played a role in the production of acid mine drainage by Colmer and Hinkle [20], the first acidophilic iron- and sulfur- oxidizing bacterium, *Thiobacillus ferrooxidans*, was isolated and described [21].

Industrial applications of bioprocessing on sulfides are conventionally divided into bioleaching and biooxidation. Bioleaching results in the solubilization of target metals (*e.g.* copper from chalcopyrite and covellite), while biooxidation refers to the microbial dissolution of pyrite and arsenopyrite associated with fine-grain gold, which can be extracted by cyanidation [22]. Besides these two metals, bioprocessing has been harnessed to extract other metals, including nickel, zinc, uranium and cobalt [23, 24]. However, today only copper and gold are the metals that are industrially produced in significant proportions by this method [18].

Bioprocessing is commercially applied in two different engineered methods: heap and stirred tank bioleaching/biooxidation. Kennecott Copper Bingham Mine has successfully used bioleaching to recover copper from run of mine material since the 1950s, which is considered as the beginning of modern commercial applications of bioprocessing. Following its lead, other mining operations around the world emerged [25]. The heap of Lo Aguirre mine, designed to facilitate the activity of the microorganisms, processed about 16,000 t copper ore/day using bioleaching between 1980 and 1996 in Chile [26]. In the mid-1980s, the first commercial plant for biooxidation of refractory gold bearing concentrate was commissioned at the Fairview operation in South Africa. Its annual gold production in 2010 was about 98 oz [1].

## **2.2 Diversity of bioleaching microorganisms**

Bioleaching processes require the regeneration of ferric ions from oxidation of ferrous ions by the acidophilic microorganisms. Most described acidophilic microorganisms were found in the acid mine drainage (AMD), which is characterized by high acidity and high levels of metals and sulfate. Despite the hostile nature of this environment, microbial communities thrive [27].

The most described acidophilic metal sulfide oxidizing microorganisms belong to the mesophilic and moderately thermophilic bacteria while archaea are usually extremely thermophilic (except the genus *Ferroplasma*) [28]. Some metal sulfide oxidizers grow facultatively autotrophically, mixotrophically, or heterotrophically, such as *Acidithiobacillus caldus*, *Thiomonas cuprina*, *Acidimicrobium ferrooxidans*, “*Ferrimicrobium acidiphilum*”, Firmicutes, *Ferroplasma*, and several extremely thermophilic Archaea. Table 1 lists the various species of acidophilic microorganisms that can grow in extremely acidic waters (pH < 3). Details on these acidophiles can be found elsewhere [27-29].

A number of studies of AMD have identified major bacterial lines of descent as divisions within the Proteobacteria, Nitrospira, Firmicutes, Actinobacteria and Acidobacteri. The Proteobacteria (formerly known as the purple bacteria) are by far the most numerous microorganisms that are known, either as isolates or as environmental clones. Acidophilic bacteria are found in three sub-groups ( $\alpha$ ,  $\beta$  and  $\gamma$ ) of this division [30]. Acidophiles within the subcategory of  $\alpha$ -Proteobacteria are predominantly heterotrophic. Some may affect mineral dissolution either via an oxidative route (by modifying the activities of iron and sulfur oxidizers) or directly via reductive dissolution. Two  $\beta$ -Proteobacterial groups have been detected to date: *Thiomonas* sp. (strains Ynys1 and Ynys3) [31] and an isolate designated NO-16 from a Norwegian mine [32].

**Table 1.** A summary of common acidophilic microorganisms.

Acidophilic species	Optimum pH	Optimum temperature (°C)	Reference(s)
<b>Iron-oxidizers</b>			
<i>Leptospirillum ferrooxidans</i>	1.5-3.0	28-40	[33-35]
<i>L. ferriphilum</i>	1.3-1.8	45-50	[36]
“ <i>Ferrimicrobium acidiphilum</i> ”	2.0-2.5	37	[37]
<i>Ferroplasma acidiphilum</i>	1.7	35	[38]
<b>Sulfur-oxidizers</b>			
<i>Acidithiobacillus thiooxidans</i>	2.0-3.0	28-30	[39, 40]
<i>At. caldus</i>	2.0-2.5	45	[41, 42]
<i>Thiomonas cuprina</i>	3.5-4.0	30-36	[43]
<i>Metallosphaera</i> spp.	2.0-3.0	70-75	[44-46]

<i>Sulfolobus</i> spp.	2.0-2.6	60-75	[47, 48]
<b>Iron-and sulfur-oxidizers</b>			
<i>Acidithiobacillus ferrooxidans</i>	2.5	30-35	[21, 49, 50]
<b>Table 1. (Continued).</b>			
<i>Acidianus</i> spp.	1.5-2.0	70-90	[51]
<i>Sulfolobus metallicus</i>	2.0-3.0	75	[52]
<b>Iron-reducers</b>			
<i>Acidiphilium</i> spp.	2.5-3.5	27-37	[53, 54]
<b>Iron-oxidizers/reducers</b>			
<i>Acidimicrobium ferrooxidans</i>	~2	45-50	[55]
<b>Iron-oxidizers/reducers and sulfur-oxidizers</b>			
<i>Sulfobacillus</i> spp.	1.6-2.5	37-55	[56, 57]

The genus *Acidithiobacillus* was proposed by Kelly and Wood [50] after reclassification of some species of the genus *Thiobacillus*. The affiliation of the genus *Acidithiobacillus* to the  $\beta$ - or  $\gamma$ -Proteobacteria is not clearly defined in the literature [30, 58]. Species of the genus *Acidithiobacillus* are obligatorily acidophilic (pH<4.0), Gram-negative, motile rods [28]. Carbon dioxide is fixed by means of the Benson-Calvin cycle. The genus comprises the following species: *A. ferrooxidans*, *A. thiooxidans*, *A. caldus* and *A. albertensis*.

*A. ferrooxidans* (formerly *Thiobacillus ferrooxidans*), an obligate chemolithoautotrophic bacterium affiliated with the Gram-negative  $\gamma$ -Proteobacteria, was the first described metal sulfide oxidizing microorganism [59]. It was commonly discovered in the bioleaching system operated at temperature lower than 40 °C [50]. *A. ferrooxidans* can accelerate the dissolution of copper sulfide by means of regenerating the ferric ions which serve as the oxidant [26]. In addition to the ferrous ions, this species can live on the oxidation of various reduced sulfur compounds such as elemental sulfur, thiosulfate, trithionate and tetrathionate. It can also grow anaerobically by respiration using sulfur compounds or hydrogen coupled with  $\text{Fe}^{3+}$  reduction [59]. To date *A. ferrooxidans* is the most intensively studied bacterium used as a model microorganism for describing the mechanism of bioprocessing.

*A. thiooxidans* belongs to the  $\gamma$ -subclass of the Proteobacteria. It is motile by means of a polar flagellum and can grow in the liquid medium on elemental sulfur, thiosulfate or tetrathionate. However, it cannot oxidize iron or pyrite but has been shown to grow on sulfur from pyrite in

co-culture with “*L. ferrooxidans*”, an iron-oxidizing, sulfur-non-oxidizing vibrio [50]. A scheme of the sulfur compound oxidation pathways was presented by Kamimura et al. [40].

Cells of *Leptospirillum* species within the Nitrospira division are helical curved rods. Isolates belonging to the *Leptospirillum* group have been obtained from AMD environments characterized by a range of temperatures and pH values. Previously, phylogenetic analysis of *Leptospirillum* sequences defined two groups, I and II [60], that have approximately 93% 16S rDNA sequence similarity. Research by Bond et al. significantly extend the diversity of the *Leptospirillum* cluster to three groups [61]. Sequences represented by group III clones have only 89 to 93% similarity to sequences from both existing *Leptospirillum* groups I and II and likely represent a new group of organisms that are yet to be isolated in culture [61]. Groups I and II are autotrophic, oxidize iron for energy, and have optimum growth temperature of 26 to 30 °C (group I) and 30 to 40 °C (group II). Group III were shown to comprise the majority of bacteria in sub-aerial slimes on the surface of a ‘slump’ of fine-grained pyrite ore [61].

*A. caldus* belonging to the Gram-negative  $\gamma$ -Proteobacteria was first described by Kelly and Harrison in 1989 [62]. Like *A. thiooxidans*, *A. caldus* grows autotrophically with various sulfur compounds and not with ferrous ions, but it has a higher optimum temperature at 45 °C. *A. caldus* can remove the extremely hydrophobic elemental sulfur building up on the mineral surface by producing surface-active agents, resulting in the enhancement of the contact of both microorganisms and ferric ions to the mineral surface. Consequently, it can accelerate the oxidation rate and minimize the formation of a sulfur layer on the mineral surfaces, which otherwise has a passivation effect on the bioleaching by iron-oxidizing bacteria [42].

*Acidiphilium* spp. fall into the  $\alpha$ -Proteobacteria and are the most commonly reported acidophilic heterotrophs in metal-rich, acidic environments. They are able to adapt to a wide range of temperature (17 °C to 45 °C) and pH values (1.5 to 6.0) [27]. Frequently, they occur as cryptic satellite organisms in cultures of iron- and sulfur-oxidizing chemolithotrophs. Phylogenetic analysis based on 16S rDNA sequences segregates currently recognized *Acidiphilium* spp. into two distinct groups. The first includes *A. cryptum*, as well as *A. organovorum* and *A. multivorum*. The second group includes *A. acidophilum* (formerly *Thiobacillus acidophilus*), *A. rubrum* and *A. angustum* [30]. The first isolated *Acidiphilium* sp. by Guay and Silver in 1975 was classified as *T. acidophilus* due to its growth with sulfur [30]. As with many other *Acidiphilium* spp., its source was a supposedly pure culture of *A. ferrooxidans*. One of the characteristics of all *Acidiphilium* spp. is their ability to reduce



ferric iron to ferrous when small amounts of oxygen are present. Among the acidophilic archaea, several genera are obligate aerobes (*Picrophilus*, *Sulfolobus*, *Metallosphaera* and *Sulfurococcus*), two genera are facultative anaerobes (*Thermoplasma* and *Acidianus*) and a single genus/species is obligated anaerobic [63]. Archaeal lineages reported from AMD environments only fall into the *Thermoplasmatales* and *Sulfolobales* [27].

## 2.3 Microscopic structures of bioleaching bacteria

### 2.3.1 Cell wall

The cell wall of Gram-positive bacteria consists primarily of the relatively uniform peptidoglycan-based layer. In contrast, the cell wall of Gram-negative bacteria (Fig. 1) presents as a highly organized outer membrane in which an asymmetrical bilayer of phospholipid and lipopolysaccharide (LPS) constitutes a permeability barrier. Diffusion pores, formed of aggregates of internal proteins, connect the periplasm of the cell to the external environment [64]. In general, compared to Gram-positive bacteria, the outer membrane of the Gram-negative bacteria makes their envelopes less permeable to a wide variety of molecules, such as hydrophobic compounds and higher molecular weight hydrophilic compounds [65].

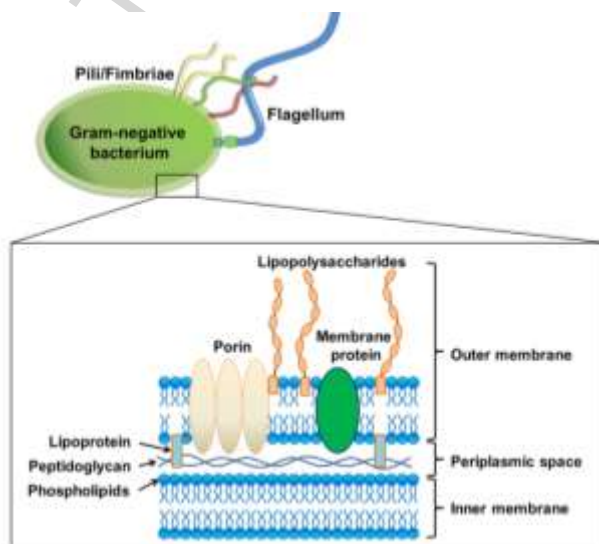


**Figure 1.** Schematic of the cell wall structure of Gram-negative bacteria with several surface appendages.

The cell wall of Gram-negative bacteria is multilayered and contains only a thin layer of peptidoglycan, which does not carry covalently-linked accessory polysaccharides or related compounds [66]. The LPS molecules are anchored to the outer membrane with significant

variations in coverage, thickness and local distribution [67]. LPS consists of a hydrophobic lipid moiety known as lipid A, a core polysaccharide and an outermost portion of O-antigen-specific polysaccharide side chain [68]. The length of LPS chains can reach up to 40 nm, depending upon the number of repeating units, bending of the O-antigen chain and the solution conditions such as pH and salt concentration [69]. LPS has been characterized in *Acidithiobacillus* species, and the effect of removal of LPS on the bacterial adhesion ability has also been reported extensively [70-72]. At least two *c*-type cytochromes binding to the membrane proteins of *A. ferrooxidans* involves in the electron transport [59]. The chemical composition of LPS (*i.e.* O-antigen type) on *A. ferrooxidans* surface can be influenced by different growth substrates, resulting in changes of cell surface charge and/or hydrophobicity, which likely affect the adhesion ability to mineral surfaces.

### 2.3.2 *Surface appendages*

Many motile bacterial species exhibit chemotactic behavior, in which the organism moves towards or away from various chemicals or stimuli. Generally, bacteria are attracted by nutrient sources and repelled by potential inhibitory or harmful agents [65]. A variety of surface appendages may project beyond the cell surface into the external environment to facilitate the cell motion and adhesion ability.

Flagella are the longest cell appendages that have been observed, extending up to 20  $\mu\text{m}$  from the cell surface for some bacteria. Some microorganisms possess very large numbers of flagella and in this case, due to their extreme rigidity and great length, they are likely to affect the closeness with which the cell can approach a surface. The arrangement of flagella on the cell surface varies between species. The flagellum has a complex basal body which permits the filament of the flagellum to rotate. This is located in the cell envelope and therefore differs in structure in the Gram-positive and Gram-negative bacteria. Gram-negative bacteria swim in a straight line with prolonged counter-clockwise rotation of the flagellum but tumble when they rotate in a clockwise fashion [65].

Many bacteria possess surface appendages in addition to the flagella, namely fimbriae and pili. Fimbriae and pili are filamentous, protein appendages which can be visualized by electron microscopy on the surfaces of a wide range of bacteria, especially Gram-negative species. A precise definition of their appearance and general characteristics is difficult since large variations in morphology and other properties are seen even between types of pili

produced by different strains of the same bacterial species [66]. The common fimbriae are smaller and more numerous than flagella and occur widely in Gram-negative bacteria and a single Gram-positive group, the *Corynebacteria*. These fimbriae are believed to play an important role in the attachment of bacteria to surfaces [66]. A special class of fimbriae, the conjugative pili, are restricted to Gram-negative bacteria, being present in low numbers per cell and appearing much longer and wider than the common fimbriae.

A single flagellum (over 1 $\mu$ m in length) and type IV pili have been found in some highly motile strains of *A. ferrooxidans* [73, 74]. Fimbriae have also been detected in *Acidithiobacillus* sp. Strain A2 [75]. The composition of the flagella protein of the *A. ferrooxidans* cell surface changed according to the culture substrate and the sulfur-grown cells show greater adhesion to sulfur than iron-grown cells [73]. According to the report of some researchers [76, 77], *L. ferriphilum* cells are Gram-negative, spore forming and motile by means of a single polar flagellum. *A. thiooxidans* is also motile by means of a polar flagellum [78] or a tuft of polar flagella [79].

### 2.3.3 Extracellular polymeric substances (EPS)

Extracellular polymeric substances (EPS) were defined as “organic polymers of microbial origin which in biofilm systems are frequently responsible for binding cells and other particulate material together (cohesion) and to the substratum (adhesion)” [80]. EPS lie outside the cell wall (peptidoglycan layer) of Gram-positive bacteria and the outer membrane of Gram-negative bacteria. The composition of EPS is highly variable even among the strains of the same species, but it is mainly composed of a mixture of macromolecules, such as proteins, polysaccharides, nucleic acids and lipids, and are often referred to as glycocalyx or slime, which facilitate bacterial attachment to the substratum [81].

After extensive studies of EPS, some general functions have been found. It has been reported that EPS play significant roles in the formation of gel-like substances, bacterial adhesion phenomenon and protection of bacterial community from toxic compounds. EPS are not necessary structures of bacteria in laboratory cultures, since loss of EPS does not impair growth and viability of the cells [81].

In the bioleaching process, microorganisms like *L. ferrooxidans* can attach to the mineral surface and develop the biofilm within a few days, covering the mineral surface with cells embedded in a continuous EPS layer. Sand and Gehrke [82] reported that the production of

EPS during bioleaching mediate the attachment of microorganisms to the mineral surfaces and the interfacial reaction of the minerals, microorganisms and the passivation layer. They claimed that the majority of cells attach to the metal sulfides by the positively charged iron (III) ion-complexed EPS layer, where the dissolution reactions occur. The zeta potential of three commonly used bioleaching bacteria, *A. ferrooxidans*, *A. thiooxidans* and *L. ferrooxidans*, were measured in iron-free 9K medium at pH 2 by Zhu et al. [83] and the results show that all these strains are positively charged with approximately 3 mV zeta potential. Similar results for *L. ferrooxidans* were reported by Vilinska et al. [84]. In contrast, Devasia et al. [85] and Sharma et al. [86] found that ferrous ion-grown *A. ferrooxidans* cells were slightly negatively charged while sulfur and pyrite grown cells were positively charged in 0.001 M KCl solution at pH 2. Blake II et al. [87] reported that when grown on sulfur, pyrite or ferrous ions *A. ferrooxidans* cells were negatively charged at pH 2. Diao et al. [88] reported that the zeta potentials of *A. thiooxidans* and *L. ferrooxidans* cells in half-strength 9K medium at pH 2 were  $-0.6 \pm 0.6$  mV and  $-2.2 \pm 2.7$  mV, respectively. The discrepancy in the surface charge of *A. ferrooxidans* might be due to the strain difference, various supporting electrolytes and different washing procedure when collecting the cells. The EPS produced by *L. ferrooxidans* and the mixture of *L. ferrooxidans*, *A. thiooxidans* and *A. ferrooxidans* after 2 h of incubation was observed by epifluorescence microscope (EFM) and the amount of attached cells and the amount of visible EPS of the mixed culture was more than that of the pure *L. ferrooxidans* [89].

**Table 2.** Different physical and chemical extraction methods of EPS used in different systems.

Methods	Samples	References
High-speed centrifugation	<i>Klebsiella aerogenes</i>	[90]
Sonication and centrifugation	Sewage biofilm	[91]
Precipitation with acetone	Supernatant of yeast culture	[92]
EDTA	Sludge	[93]
Heating to 70 °C	<i>Rhodopseudomonas acidophila</i>	[94]

To understand the functions of EPS, its chemical composition should be analyzed. Table 2 summarizes several methods for isolating EPS from various samples, which can be classified

into physical or chemical methods or their combination. An intensive review paper about EPS extraction and analysis can be found at [95]. EPS of various bioleaching microorganisms were isolated and characterized by different research groups. The extracted EPS were analyzed for nitrogen, uronic acids and protein [96, 97]. Sand and Gehrke [82, 96] reported that the molar ratio of uronic acids and ferric ions within the EPS of *A. ferrooxidans* and *L. ferrooxidans* is about 2:1, resulting in a net positive charge of cells. In the acidic leaching solutions, many sulfide minerals have a net negative charge. Therefore, the positive-charged bacteria can attach to the negative-charged mineral surface due to the electrostatic forces [97]. The macroscopic adhesion experiments reported by various groups are in agreement with the chemical analysis of EPS. The adhesion experiment reported by Zhu et al. [83] demonstrates that the removal of EPS causes a significant reduction in cell attachment. Xia et al. [98] reported that the sulfur-grown *A. ferrooxidans* cells show higher affinity to the chalcopyrite surface than that of ferrous ion- and chalcopyrite-grown cells within 60 min. The amount and composition of EPS produced varies due to many reasons, such as the differences of bacterial strains, the culture media and the incubation time. Zeng et al. [97] reported that the amount of EPS extracted from a mixed culture of moderately thermophilic microorganisms cultured with chalcopyrite concentrates increased quickly and stabilized until the end of bioleaching, but the molar ration of uronic acids to ferric ions varied with the bioleaching time. It is proposed that the EPS fills the void between the outer membrane of cells and the mineral surfaces [82]. However, this process has not been elucidated in detail.

#### **2.4 Macroscopic cell surface properties**

The adhesion behavior of bacterial cells is governed by the cell surface physicochemical properties as well as the interactions between the macromolecules and solid substrates [99]. The electrical potential and hydrophobicity are considered to play an important role in the bacterial adhesion.

The contact angle measurement techniques are commonly used for the abiotic surfaces for studying the colloidal systems. To assess the bacterial surface free energy, the contact angle measurement of probe liquids on the bacterial lawn is the most commonly used method. Sharma and Rao [100] reviewed different theories for evaluation of surface energy of 140 microbial strains by contact angle measurements. Among various approaches giving different predictions, the Lifshitz-Van der Waals and acid-base (LW-AB) model provides the most

detailed information about the microbial cell surface and can predict the attachment of bacterial adhesion to solid surfaces [16, 101, 102].

The measurement of contact angle for bacterial cells is conducted by producing an uniform layer of cells on agar surface or a bacterial lawn deposited on membrane filters [7]. The deposited bacterial lawn method is preferred because cells on the membrane can be dried to allow only bound water to be present on the cell surfaces. Busscher et al. [7] reported the detailed method for the preparation of a bacterial lawn and contact angle measurement. Concisely, bacterial cells were harvested and washed before being collected on a membrane filter by vacuum filtration. Specifically, some authors reported an estimation of the number of cell layers deposited onto the membrane to insure that cells completely and homogeneously covered the membrane [7, 103]. A drop of probing liquid is placed on the cell surface, and the contact angle is taken with a sessile drop method.

However, predictions for the adhesion behavior of bacteria in terms of hydrophobicity and surface free energy are not ubiquitously successful. Several reasons relate the limited success: 1) The soft nature and the heterogeneity of bacterial cell surfaces due to the presence of various biopolymers and cell surface appendages, such as flagella and pili, which deviate the bacterial surface behavior from that of rigid colloidal particles [101]. 2) The contact angle results can be easily affected by experimental variations such as the distinct moisture content of the bacterial lawn, incomplete coverage on the membrane and differences in the time recorded for the contact angle measurement [100].

Hydrophobicity of microbial surfaces can also be estimated from the MATS (microbial adhesion to solvents) tests [104]. This partitioning method is based on the bacterial liquid-liquid partition into hydrocarbons such as *n*-hexadecane, *n*-octane or *p*-xylene [105]. The surface hydrophobicity of bioleaching bacteria has been widely studied by means of contact angle measurement [2, 84, 88, 106] and the MATS tests [85, 107, 108]. Although the values of contact angle vary from one strain to another, but all the data demonstrate that bioleaching bacterial surfaces are hydrophilic.

Most microorganism surfaces are negatively charged under physiological conditions due to their negatively charged surface functional groups such as amino, carboxyl and phosphate groups. The net cell surface charge can be estimated from the zeta potential which is the electrical potential of the interfacial region between the bacterial surface and the aqueous

environment. The zeta potential can be calculated from measured microbial electrophoretic mobilities in an electric field using different approaches such as the Smoluchowski equation and the soft-particle theory [109]. In addition, bacterial surface charge can also be determined by proton titration [110] and dielectric spectroscopy [111].

Besides the complex and highly dynamic nature of bacterial cell surfaces, charged functional groups on the cell surface may associate upon the changes of pH and the ionic strength of the supporting solutions. The conformation of cell surface biopolymer chains and ultrastructural appendages may be affected by the changes in ionization states of the functional groups. In addition, the surface charge of bacterial cells varies according to bacterial species and can be affected by the growth substrate and growth phase. The zeta potentials of various bioleaching microorganisms in different aqueous solutions have been reported by many researchers. The isoelectric point of these acidophiles is between pH 2 and pH 3.5 [86, 106]. Many reports compared the zeta potentials of mineral surfaces before and after interaction with bioleaching microbes. The results indicate that the attachment of bacterial cells onto mineral surfaces can alter the surface electrochemical properties of mineral particles [85, 107], *e.g.* the IEP of mineral particles shift to the IEP of bacterial cells.

## **2.5 Bacterial adhesion mechanism in the interfacial process of bioleaching**

The bacterial adhesion can be influenced by physiochemical and biological factors, such as the hydrophobicity of bacterial cell and substratum surfaces, strength of cell-substrate interacting forces, the time development of adhesive contact, solution conditions (pH and ionic strength), and the culture age and growth conditions [112-114].

The attachment of bacterial cells to surfaces can be distinguished in various steps: 1) transport of bacterial cells to the surface; 2) initial adhesion; 3) firm attachment; 4) surface colonization [115]. In the first step, bacterial cells can approach the surface through different mechanisms, such as diffusive transport, fluid convective, sedimentation and cell motility. During the approach of bacteria to solid surfaces, various interfacial forces govern the cell attachment process which will be discussed later in the review. The next step is the initial adhesion. An extensive overview of physicochemistry of initial bacterial adhesion interactions is given by Bos et al. [116]. The initial adhesion can be generally distinguished into reversible and irreversible. The following step is the firm attachment. Typically, after the bacteria deposit on the surface the chemical processes occur will lead to changes in the in

molecular composition of the cell surface. For example, the cell may increase the production of LPS, surface proteins or other extracellular polymeric substances, which have been shown to be essential for the development of biofilms [97]. On the other hand, the surface structures and appendages may form strong links between cells and the solid surface. Finally, the bacterial cells must form a strong interaction with the solid surface to resist dislodgement from the surfaces. The last step of the microbial adhesion is attributed to the growth of attached cells and attachment of newly formed cells to each other in the biofilms [115].

The interactions between microorganisms, mineral surfaces and the leaching solutions in a bioleaching system are illustrated in Fig. 2. Over the last 40 years there has been a long-standing debate concerning the mechanism of bioleaching, the so-called direct and indirect mechanisms. In recent years there is a growing consensus view that the bioleaching mechanism can be proposed as non-contact, contact and cooperative leaching [117]. In the non-contact mechanism, a chemical attack by ferric ions or protons on a mineral sulfide resulting in the dissolution of the mineral and the generation of ferrous ions and various forms of sulfur compounds. The ferric ions can be regenerated by the planktonic iron-oxidizing microbes by re-oxidizing the ferrous ions as the electron donor. The mechanism of bacteria interaction with pyrite is described as follows:

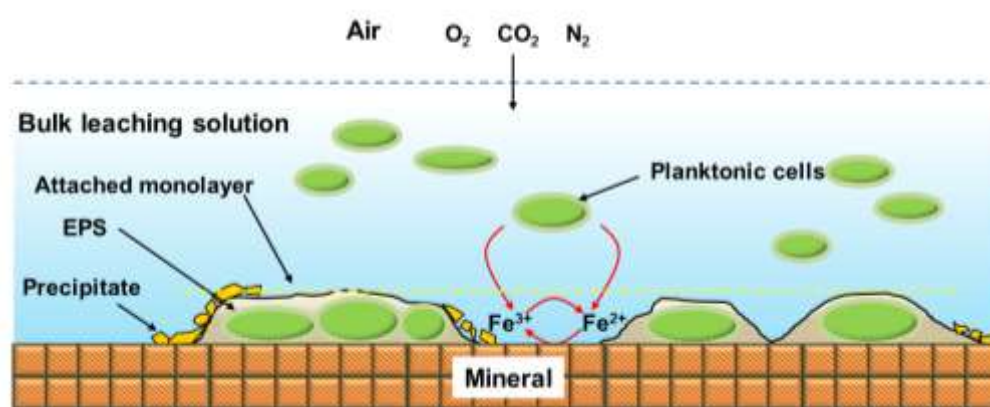
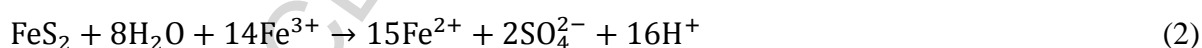
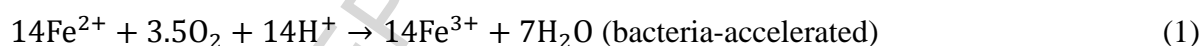


**Figure 2.** Schematic of bacteria-mineral interactions in a bioleaching system.

The contact mechanism refers to the attached bacterial cells on the mineral surfaces with the EPS layer serving as reaction space for the oxidizing of ferrous ions. The dissolution of



sulfide minerals takes place at the interface between bacteria cell and the mineral surface. The localized corrosive bacterial action resulting in cell-sized pits on a sulfide mineral has been observed [118]. However, there are still some debates on the formation of these corrosive pits, which is due to the chemical attack in the non-contact mechanism.

For metal sulfides that cannot be dissolved in acid solution, some bacteria attach to the mineral surface while other planktonic bacteria cooperate the oxidative dissolution during the bioleaching process, namely cooperative leaching [119]. Bacteria can adhere to mineral surfaces by the electrostatic attraction and/or hydrophobic interaction. After the encounter of bacteria and mineral surfaces, bacteria may adhere to the surface by secreting polysaccharide or with the assistance of surface appendages. Subsequently, microbes will grow and reproduce resulting in the formation of micro-colony or biofilm. A highly packed arrangement of *A. ferrooxidans* on synthetic pyrite surface was observed using scanning electron microscopy (SEM) [120]. The pH value of leaching solution is of great importance to the bacterial activity as well as in the prevention of formation of a passivation layer (*e.g.* jarosite) which inhibits the nutrient source of the bacteria and the dissolution of the mineral.



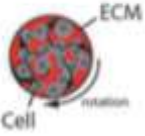
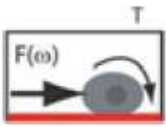
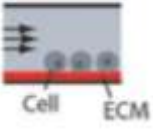
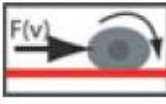
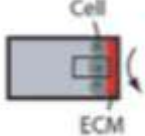
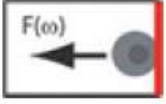
### **3. Applications of AFM in bacterial adhesion research**

The preceding discussion indicates that much attention has been given to the macroscopic properties and the measurement of large ensembles of cells by means of zeta potential and contact angle measurements. Moreover, the bacteria-substrate adhesion force has been widely investigated by various approaches (*e.g.* flow chambers and spinning disks) using the shear force to detach the adherent bacterial cells and measure the lateral detachment force. An overview of bulk adhesion assays (Table 3) is provided by Taubenberger et al. [121]. However, the disadvantages including low sensitivity and precision and time-consuming sample-preparation procedure limit the application of these methods in measuring the interaction forces.

In order to better understand the fundamental forces governing the bacteria-solid interactions, the magnitude of forces is directly quantified by mean of various surface force apparatus, among which the AFM exhibits its versatility over other instruments. Since its invention by Binnig et al. in 1986 [122], it has developed into a powerful tool for topographic imaging in air and liquid conditions and in measuring the interaction forces at nanoscale. Compared to the electron microscope techniques, AFM is advantageous in probing the three-dimensional

topography and quantifying the interactions forces for both conducting and non-conducting materials, such as biological samples, in air and fluid environments [123].

**Table 3.** Overview of commonly used bulk adhesion assays to cell adhesion [121].

Assay	Force application	Read-out
 Cell	Uneven/unknown shear forces	 Direct counting for ratio of attached/non-adherent cells
 Cell ECM rotation	Shear forces (force gradient)	 Disc radius at which 50% of cells remained attached (shear forces estimated)
 Cell ECM	Shear forces (laminar flow)	 Ratio of attached/non-adherent cells; analysis of rolling cells (binding frequency and arrest time)
 Cell ECM	Centrifugal force	 Number of attached cells

schematic description of the principle is shown on the left. F, force; v, velocity;  $\omega$ , angular velocity.

AFM can be used to probe the interaction forces, such as van der Waals, electrostatic, double-layer and capillary forces, between surfaces or molecules. The plot of the force as a function of the tip-sample separation is briefly called a force curve, providing better understanding on sample properties such as elasticity [124], Hamaker constant [125], adhesion [16] and surface charge densities [125]. For this reason the measurement of force curves has become essential in different fields of research such as surface science, materials engineering and biology [126].

### 3.1 Principles of AFM

The heart of an AFM instrument is a tipped or tipless micro-fabricated cantilever. As the tip scans over the surface of interest, the interaction forces between the tip and the sample surface cause deflection of the cantilever according to Hooke's law. By monitoring the

deflection of the cantilever a topographic image of the surface can be built up to a high resolution [127].

The deflection of the cantilever is determined by the displacement of the laser beam on the photodetector. The photodetector is segmented into four parts, and a voltage is generated from each quadrant which is proportional to the amount of light hitting it. Normally the laser beam is aligned to center the spot on the photodetector when the cantilever is undeflected. The more the spot moves at the detector, the more signal is generated. The intensity of the signal is called the optical lever sensitivity (OLS).

There is a broad range of AFM cantilevers made out of different materials. Silicon and silicon nitride ( $\text{Si}_3\text{N}_4$ ) are two extensively used materials for fabricating AFM cantilevers. They have two shapes: rectangular (diving board shaped) and triangular (“V”-shaped). The cantilever has a sharp tip at its end, which is commonly in the form of a pyramid or a cylindrical cone. The geometry of the cantilever tip is a crucial parameter in AFM force measurement if the experimental force data are fitted in theoretical models. However, the geometry of the tip is difficult to determine, and the shape of the tip can change over time. To solve this problem, one can periodically characterize the tip with an electronic microscope or the tip can be replaced by a microsphere by the colloidal probe technique [128].

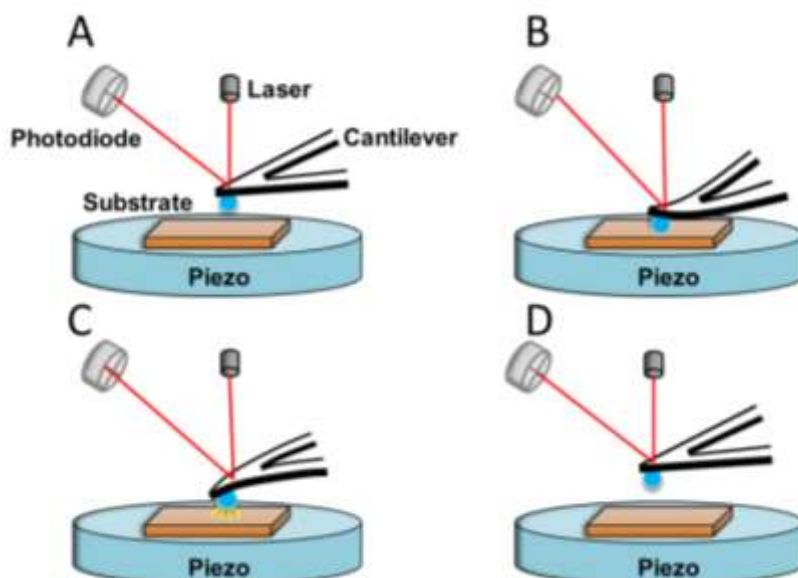


**Figure 3.** Schematic of an atomic force microscope and a force measurement cycle.

AFM scanners are made from piezoelectric material, which expands and contracts proportionally to the applied voltage. In the force measurement, the sample is mounted onto the scanner and moved in x and y directions by the piezoelectric translator. In some AFM instrument, the chip is moved by the piezoelectric translator instead of the sample.

Fig. 3 depicts a typical force measurement cycle using a colloidal probe. A tipless cantilever with a (functionalized) microsphere attached to the end is lowered toward the substrate surface (*e.g.* polished mineral surface). The probe senses no interaction forces when it is far away from the substrate surface (Fig. 3A). The probe keeps approaching the substrate until a preset force is reached (Fig. 3B) and then the probe is withdrawn (Fig. 3C) until complete separation from their mutual contact (Fig. 3D).

### 3.2 Immobilization of bacterial cells

AFM can be used to measure a variety of forces such as electrostatic interactions [13], van der Waals forces, hydration/hydrophobic forces [15, 129] at short distances (between 0.1 and 0.5 nm) and elastic forces [130]. The so-called adhesion forces are usually measured in the retraction phase of the force curves and have typically a magnitude between  $10^{-9}$  and  $10^{-7}$  N [131]. The total force measured for a specific biological interaction reflects the sum of all contributing interactions. Most of the force measurements between bacteria and solid surfaces are carried out *in situ* (aqueous environment). However, the application of AFM in microbiology is challenging due to the difficulty of immobilizing bacterial cells to a surface without affecting the cell surface properties or cell viability.

To measure the interaction forces in the nano- to pico-Newton range between the bacterial and substrate surfaces, two common approaches have been applied to immobilize cells. The first approach is to immobilize bacterial cells onto a planar substrate surface and use the (functionalized) AFM cantilever to touch the cell surface. The second approach is to directly attach a single cell or multiple cells to a cantilever. To obtain a true and reliable interaction force between bacterial cells and the substrate in various experimental conditions, correctly selected method for cell immobilization is of great importance. A number of methods to immobilize bacteria to a substrate in living or dead states, including mechanical entrapment, physisorption, covalent binding and immobilization with adhesive proteins, are reviewed and compared by Kuyukina et al. [11] and Meyer et al. [132].

Living yeast cells were entrapped in pores of a microfilter [133] and embedded in 3% agar gel [134]. Compared to the microfilter, the agar gel is a deformable immobilization matrix, so that allows the growth of embedded cells. One disadvantages of this method are that the molten agar at its melting point (45-50 °C) could adversely affect the viability of the deposited cells [135].

In addition to the mechanical entrapment, physisorption of the negatively charged cells by the electrical attraction from the positively charged polymer layers is commonly used for imaging and force measurements. The gelatin or poly-lysine coated mica surfaces were used for immobilization of both Gram-positive and Gram-negative bacteria in air and liquid environments [136]. Chemical fixative gives good results in AFM image comparing to drying samples on the mica surface. Dorobantu et al. [15] measured the force between chemically functionalized AFM tips and two bacterial species, *Acinetobacter venetianus* and *Rhodococcus erythropolis*, which were strongly immobilized onto the surface of glass slides coated with 3-aminopropyltrimethoxysilane.

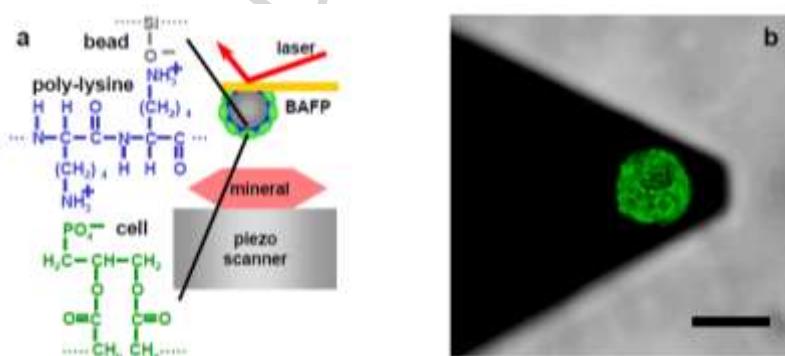


**Figure 4.** (a) Schematic of the biological force microscopy showing one of many possible poly-lysine linkages between negatively charged silanol groups on the bead and negatively charged cell-surface functional groups on biomolecules. (b) Scanning laser confocal micrograph of a biologically-active-force-probe (BAFF) [137]. Scale bar 10  $\mu\text{m}$ .

Instead of immobilizing bacterial cells onto a flat surface such as a glass slide, mica and silicon oxide, some researchers bonded the microbial cells onto the cantilevers. Various “glues” have been used, but the bacteria surfaces can be artificially altered by the external agents [138]. In 1998, Bowen and co-workers [139] reported the first use of “cell probe” to measure the adhesion force between the cell and a mica surface in a liquid cell. They picked and glued a living yeast cell onto a tipless cantilever with the poly-lysine and cyanoacrylate

glues. Kang et al. [140] also developed a method for constructing live bacterial cell probes for AFM. They used the bioinspired polydopamine wet adhesive to link the *E. coli* and yeast cells to the cantilevers and compared the force curves between viable cells and glutaraldehyde-fixed cells. Based on the bioinspired polydopamine method, Beaussart et al. attached a single bacterial-coated bead to a cantilever using a small quantity of epoxy resin, which has previously been found to be inert in aqueous solutions [123]. Lower et al. [137] used AFM to measure the interfacial and adhesion forces by linking living and unmodified *E. coli* cells to a glass bead functionalized with poly-D-lysine and formed a monolayer of cells stably attached to the bead. The force-sensing probes were fabricated by gluing the minute bacteria-coated glass bead to a silicon nitride cantilever as shown in Fig. 4. The interaction forces between living *E. coli* cells and mineral surface of muscovite, goethite and graphite were directly measured *in situ*. They also applied this method on living *Shewanella oneidensis* bacteria to investigate the interaction forces between the bacteria and goethite ( $\alpha$ -FeOOH).

Following the early work of Razatos et al. [141], glutaraldehyde-fixed bacterial cells were linked to the polyethyleneimine (PEI)-coated cantilevers by many research groups. Sheng et al. [142] immobilized anaerobic sulfate-reducing bacteria (SRB) to silicon nitride tip cantilever and measured the adhesion forces between the cell probe and four polished metal substrates. The same method was also successful in immobilization of *E. coli* cells for various force measurements [12, 143]. Only a few studies regarded the immobilization of acidophilic bioleaching microorganisms. *A. ferrooxidans* cells were attached to the PEI-coated glass slide, and the interacting forces between a  $\text{Si}_3\text{N}_4$  cantilever and the cell was recorded in difference salt concentrations and pH conditions [5]. Zhu et al. [83] constructed a cell probe by immobilizing three strains of bioleaching bacteria to the tip of a cantilever and measured the adhesion forces between bacteria and the chalcopyrite surface. Due to the small area of the cantilever tip, it is very difficult to guarantee complete coverage of the apex of the tip. To avoid recording the false interaction force between the tip and the substrate, Diao et al. [88] used the bacterial colloidal probe technique to obtain the real interactions between *A. thiooxidans*, *L. ferrooxidans* and pyrite surfaces.

All the methods mentioned above have their own pros and cons with respect to 1) ease of sample preparation; 2) reproducibility; 3) living/dead state of cells; 4) applicability to difference cells types and various aqueous environments (*e.g.* ionic strength and pH). A

correct choice of immobilization method that is most appropriate for one's experimental set-up is of great importance in the investigation of bacteria-solid interactions.

### 3.3 Applications of AFM in bioleaching research

#### 3.3.1 AFM imaging

AFM can be operated in air or aqueous medium, which allows the biological samples to be investigated in the natural environment and avoid denaturation. Several AFM imaging modes are available for topographic analysis, providing a wide range of information about the surface of interest. Imaging modes differ mainly in the way the tip moves over the sample and can be categorized into contact mode and non-contact mode, which are most commonly applied in the analysis of biological samples. At large separations, there are no interaction forces between the probe and the sample surface. As the probe and sample surface approach each other, the attractive van der Waals force and repulsive forces will occur, which cause the cantilever to deflect, and the four-quadrant of photodetector can records the position of the reflected beam.

The contact mode is commonly used to measure the topography of relatively hard surface. In this mode, the tip of the cantilever remains in continuous contact with the specimen surface while scanning across the sample surface. The topographic images are generated directly using the deflection of the cantilever. However, the contact mode of imaging will cause high shear forces, which can damage the delicate biological samples for instance or even remove the sample from the substrate if not sufficiently immobilized [135]. In the tapping mode, the cantilever is oscillated at a given frequency allowing the tip of the probe to only touch the sample surface at the end of its downward movement. In this case, the damage to the soft sample will be remarkably reduced while the probe is scanning over the surface.

Imaging for inorganic surfaces is less complicated than that for biological surfaces because inorganic surfaces have several advantages over biological samples with respect to measuring surface forces accurately. Firstly, inorganic surfaces can be cleaned more easily, *e.g.* by chemical treatment or heating. Secondly, they are harder and do not deform much under the influence of the tip. In addition, the tip often picks up some material after contacting with the biological samples. This completely changes the surface forces in an unpredictable manner [144].

AFM has been applied to image a variety of biological samples, including 1) macromolecules such as DNA, proteins and biopolymers [145]; 2) bacterial biofilms [146-149] and 3) bacteria and their appendages [150]. Scanning the sample in air is a simple and suitable approach to observe the ultrastructural appendages of bacterial cells such as the fimbriae and pili. Francius et al. [150] demonstrated the presence/absence of the surface appendages on the surface of four strains of *E. coli* and the differences in the length and thickness of the surface appendages and protein layer using the contact mode of AFM in air (Fig. 5).

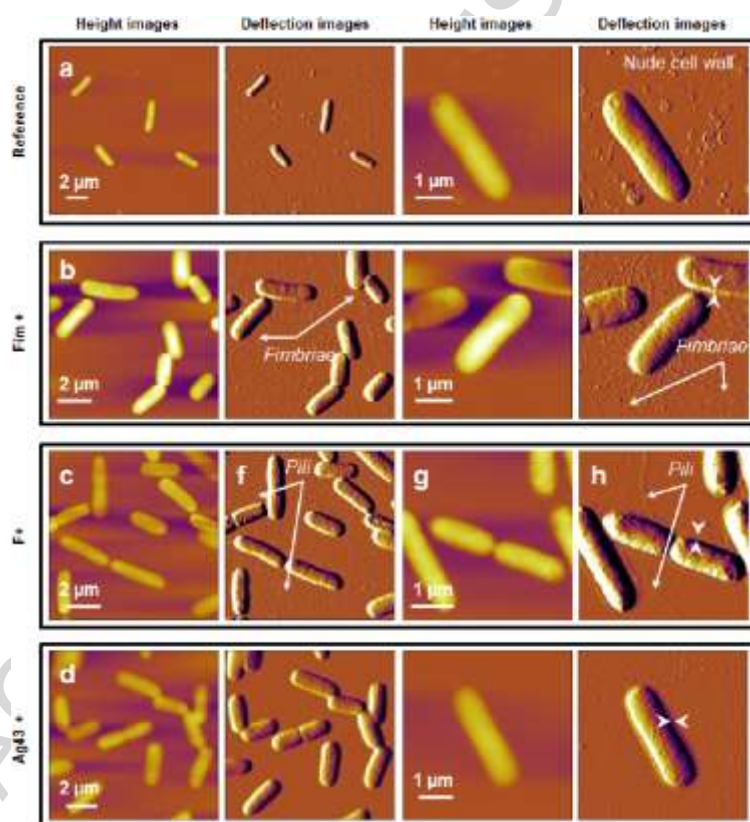


**Figure 5.** Bacterial morphology observed by the contact mode of AFM in air. AFM height and deflection images of four strains of *E. coli* (a. E2152; b. E2146; c. E2302 and d. E2498) acquired in air shown in height and deflection images with a z-scale of 200 nm [150].

The topic of living-cell imaging was intensively reviewed in [9]. Imaging under the natural environment of the living cells will be significant and necessary for determining many important properties of bacteria, such as the function and dynamics. Using the AFM equipped with biological fluid cell, the composition and temperature of the liquid media can mimic the natural environment, and the bacterial cells can be imaged in situ.



AFM is also considered as an important tool for structural molecular biology, especially for the investigation of the structure of biological macromolecules. DNA was one of the first biopolymers imaged by AFM. Lyubchenko et al. [151] obtained the AFM images of intact  $\lambda$  bacteriophage genome and several  $\lambda$  restriction fragments binding to chemical modified mica surface both in the air and liquid environments. Hansma et al. [152] investigated the images of DNA in propanol, dry helium and other aqueous buffers under the tapping mode of AFM. They obtained the best resolution in propanol due to the elimination of contact forces. Imaging of proteins, including globular proteins, fibrous proteins, cytoskeleton proteins and antibodies, have extensively studied with AFM over the past 20 years [153]. Among a variety of immobilization methods for proteins, the most commonly used approach is to chemically bond the protein to the substrate. Glass, mica, gold and silicon oxide surfaces can provide excellent support for biomolecules by allowing physical adsorption or chemical fixation onto these flat surfaces [154]. Yang and co-workers [155] imaged the pertussis toxin using AFM by attaching pertussis toxin on the mica surface. The protein solution of 15  $\mu\text{L}$  was applied to a fresh cleave mica surface and incubated for 30 min. The spatial structure of the subunits of pertussis toxin down to 0.5 nm was clearly revealed. Polysaccharides are vital structural components of all living organisms. Polysaccharides secreted by bacteria are of great importance in their adhesion to surfaces, formation of biofilms, protecting the cells from harsh environments and mediating cellular recognition [10]. A review paper on probing the properties of polysaccharide with atomic force microscopy can be found in [156].

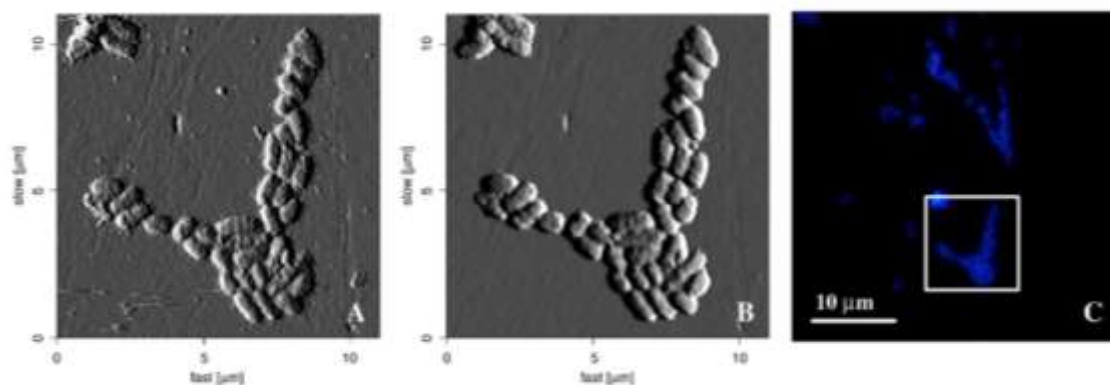


**Figure 6.** AFM and EFM image of *A. ferrooxidans* cells attached to pyrite. A: Vertical deflection image obtained by contact mode in air. B: Vertical deflection image acquired with tapping mode in mineral salt solution. C: EFM image of the same sample location [148].

In the early attempts of imaging the bioleaching bacteria attached on the mineral surface, Gehrke et al. [96] obtained an AFM image of *A. ferrooxidans* cells attached to a defective area of pyrite under contact mode. *A. ferrooxidans* cells attached on the surface of research-grade chalcopyrite at different incubation time were imaged in air using tapping mode by Bevilaqua and co-workers [157]. They found that the biofilm is evident according to the AFM images taken in the late incubation stage. Mangold et al. [148] utilized AFM to visualize the attached *A. ferrooxidans* on pyrite coupon by contact mode in air or intermittent contact mode (tapping mode) in mineral salt solution (Fig. 6). Noël et al. [149] imaged the attached *A. ferrooxidans*, *L. ferriphilum* and *A. caldus* on the pyrite coupon with the combination of AFM and EFM. They found that *L. ferriphilum* not only causes aggregate formation but also increased attachment of cells. Florian et al. [158] applied AFM and EFM to image the mixed culture of *A. ferrooxidans* and *A. thiooxidans*, and they found that the mixed culture showed a higher tendency to form aggregates on the pyrite coupon and produced more EPS. Becker et al. [159] imaged the *Sulfobacillus thermosulfidooxidans* attached to pyrite surface using in situ tapping mode of AFM, and they reported that the thickness of EPS changed with a decreasing pH.

AFM has not only successfully been applied in imaging the topography of individual cells but also bacterial biofilms on solid surfaces in air or liquid environments [146]. A biofilm is a complex aggregation of microorganisms in which cells adhere to each other and grow on all kinds of materials, including metals, plastics, soil particles, biological tissues and implant materials. The continuous biofilm formed by the Gram-negative bacterium *Azospirillum brasilense* on the polystyrene substrate was imaged by van der Aa and co-workers in situ [160]. They found that the biofilm present only under favorable conditions of the bacterium. They also carried out the adhesion force mapping over a  $5 \times 5 \mu\text{m}$  area between the biofilm and a silicon nitride tip and obtained the magnitude of adhesion force of  $0.2 \pm 0.2 \text{ nN}$ . The biofilms formed by two strains of biodeterioration on the stainless steel surface were investigated by Steele and co-workers using the non-contact mode with  $\text{Si}_3\text{N}_4$  cantilevers [147]. They observed significant deterioration of pitting corrosion formed on the steel surface caused by a mixture of two strains of sulfate-reducing bacteria. González and co-workers [161] successfully applied AFM to image the colonization process of biofilms produced by *A. thiooxidans* on the surface of pyrite. They found that the colonization began after one hour, and the initial adhesion force was about 8.1 nN from the biofilm assay.

### 3.3.2 AFM force measurements

AFM has been used to investigate the bacterial adhesion in different realms, including pathogenic microbial adhesion to biomaterials [162], bacteria adhesion to mineral surfaces [163] and biocorrosion caused by SRB [142]. The raw data recorded by AFM is a measure of the deflection of cantilever versus the piezo movement. The raw data can be converted to force versus separation distance with a known sensitivity and the spring constant of the cantilever [128]. A variety of interfacial properties can be extracted from the force-separation curves, such as the adhesion/repulsive forces, elasticity of macromolecules and nanomechanical properties of bacterial cells. A survey of AFM force measurements is summarized in Table 4. Several intensive reviews on the application of AFM in microbiology are recommended [10, 164-166].

Interactions between bacteria and mineral/metal surfaces are central to microbial attachment which results in metal corrosion, mineral bioprocessing and crystal growth. The interactions of *Shewanella putrefaciens* with Fe-coated and uncoated silica glass surface in air or aqueous solution were investigated by Grantham et al. [167]. It was found that the adhesion forces of bacteria were stronger in nutrient-depleted solutions and the adhesion forces are stronger between the bacteria and Fe-coated surface than uncoated silica glass surface. The interaction forces between a strain of SRB and mica surface were studied by Fang et al. [168], who reported that the range of forces between AFM tip ( $\text{Si}_3\text{N}_4$ ), and cell was from -3.9 to -4.3 nN (attractive) while the force between cells is stronger. Sheng et al. [142] studied the interactions between anaerobic sulfate-reducing bacteria and polished metal surfaces (*i.e.* stainless steel, mild steel, aluminum and copper) using bacteria attached probe. They found that the adhesion forces were influenced by the electrostatic force and the hydrophobicity of both metal and bacterial surfaces. The SRB showed the strongest adhesion forces to aluminum and strong electrostatic repulsion between bacterial cells.

Chandraprabha et al. [5] investigated the interaction between *A. ferrooxidans* and the AFM tip ( $\text{Si}_3\text{N}_4$ ) in different pH, ionic strength and compared the experimental force data with classical DLVO model and steric model. A repulsive force was observed at the separation of 50~60 nm when the tip approached the cell surface. The repulsive distance decreased from 120 nm to 60 nm as the ionic strength increased from 0.001 M to 1 M. By fitting the approaching curves to the steric model, the length of the polymer brush layer on the cell surface was calculated as 176.7 nm and 8.512 nm at 0.001 M and 1 M, respectively. The

interaction between the sulfur-oxidizing *A. thiooxidans* and the pyrite surface (massive pyrite electrode) was investigated by Lara and co-workers [169] using AFM with a silicon nitride cantilever. They observed a monolayered biofilm formed on the pyrite surface and adhesion force was strong (467 nN). Zhu et al. [83] measured the adhesion force between *A. ferrooxidans*, *A. thiooxidans*, *L. ferrooxidans* and chalcopyrite surfaces. The magnitude of the adhesion force was between 0.5 to 1 nN. They also found that the magnitude of adhesion forces slightly decreased after EPS removing for these bacteria. Diao and co-workers [170] compared the adhesion behavior of *A. ferrooxidans* and *A. thiooxidans* on chalcopyrite surface. They reported that the magnitude of adhesion force and snap-off distance of these bacteria is remarkably influenced by the solution pH. In addition, *A. ferrooxidans* cells exhibit a stair-step retraction pattern, while *A. thiooxidans* cells display a saw-tooth shaped separation curve.

**Table 4.** Bacteria-surface interactions probed by atomic force microscopy technique.

Method	Microbe	Substrate(s)	Cell immobilization	Results	Reference(s)
Force-separation curves with single cell/multiple cell-coated probes	<i>E. coli</i>	Mica, hydrophilic/hydrophobic glass, polystyrene and Teflon	Glutaraldehyde+PEI coating	Steric forces, hydrophobic interactions and DLVO forces	[12]
		Muscovite, goethite and graphite	Poly-D-lysine coating	Attractive hydrophobic forces, repulsive solvation, steric forces and adhesion forces	[137]
		Quartz	Polydopamine coating	Repulsive steric forces and multimodal adhesion forces	[140]
		Hematite and corundum nanoparticles	Gelatin-coating	Adhesion forces and elasticity of cells	[171]
		Fluorosilane, aminosilane, mica, PEG and unmodified silicon wafer	Poly-L-lysine coating	Adhesion forces, electrostatic interactions and hydrophobic attraction	[172]
	Bioleaching bacteria ( <i>A. ferrooxidans</i> , <i>A. thiooxidans</i> and <i>L. ferrooxidans</i> )	Chalcopyrite	Glutaraldehyde+PEI coating	Adhesion forces and electrostatic interactions	[83]

**Table 4.** (Continued).

Method	Microbe	Substrate(s)	Cell immobilization	Results	Reference(s)
	<i>A. thiooxidans</i> and <i>L. ferrooxidans</i>	Pyrite and silica wafer	Glutaraldehyde+PEI coating	Adhesion force and stretching of biopolymer chains	[88]
	<i>Lactobacillus plantarum</i>	Lectin-coated glass and 1-dodecanethiol/11-mercapto-1-undecanol coated glass	Polydopamine coating	Adhesion forces	[123]
	<i>Pseudomonas aeruginosa</i>	Clean glass slide	Poly-D-lysine coating	Adhesion force and viscoelasticity of biofilm	[173]
Force-separation curves with bare/functionalized silicon nitride probes	<i>E. coli</i>	Bare silicon nitride probe	PEI coated glass	Elasticity of cell wall, analysis of Turgor pressure and stretching of surface appendages	[150]
	<i>Klebsiella pneumoniae</i>	Bare silicon nitride probe	PEI or gelatin coated glass	Steric forces, electrostatic interactions and elasticity of cell wall	[174]
	<i>Acinetobacter venetianus</i> and <i>Rhodococcus erythropolis</i>	Alkanethiols terminated with hydroxyl or methyl groups coated silicon nitride probe	3-aminopropyltrimethoxysilane coating	Attractive hydrophobic interactions, repulsive hydration effects and steric interactions	[15]
	<i>A. ferrooxidans</i>	Bare silicon nitride probe	PEI coated glass	Steric repulsion and electrostatic interaction	[5]

Ong et al. [12] measured the interaction forces between *E. coli* cells and different materials, including mica, hydrophilic or hydrophobic glass, polystyrene and Teflon. The force measurements were carried out using an *E. coli* cells coated probe and the measured forces were compared to the extended-DLVO model. They reported that the adhesion of *E. coli* cells is enhanced by the surface hydrophobicity of the substrate and the experimental data of strains with short carbohydrate chains on the outer surface agreed well with the theoretical predictions. Van der Mei and co-workers [175] reported the direct measurement by atomic force microscopy of the surface softness of a fibrillated and a nonfibrillated oral bacterial strain. The results show that a long-range repulsion force existed when the AFM tip approached the fibrillated strain, and the nonfibrillated strain was stiffer than the fibrillated strain in water.

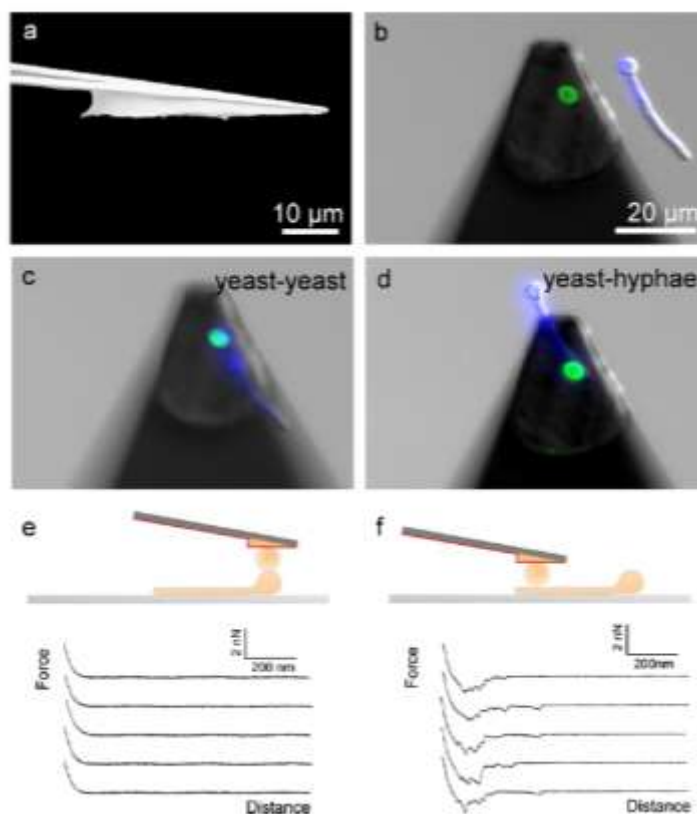


**Figure 7.** Force spectroscopy of cell-cell interaction using wedged cantilevers. (a) SEM image of a wedged cantilever. (b) A cell probe (labeled with green Con A-FITC) prepared from a nondestructive method approached a *C. albicans* hyphae (Calcofluor White, blue) which was immobilized on a hydrophobic substrate. The yeast cell probe was positioned on top of the yeast region (c, e) or the germ tube region of the hyphae (d, f) with the corresponding representative force-distance curves (e, f) [176].

Recently, based on the single-cell force spectroscopy (SCFS) technique [123] Alsteens et al. quantified the interaction forces between the yeast cell and hyphae of the fungal pathogen *Candida albicans* by a wedged cantilever (Fig. 7) [176]. Force-distance curves showed strong, short-range adhesion peaks followed by weak, long-range tether adhesion events, which originate from specific cell surface proteins. These force measurement results provide novel insights into the molecular origin of the cohesive strength of fungal biofilms.

### 3.3.3 Nanomechanical properties

AFM indentation has become an important technique for quantifying the mechanical properties of living cells. The cell elasticity modulus can be determined from the force curves measured in AFM indentations. Yao et al. [177] measured the elasticity of sacculi from Gram-negative bacteria *E. coli* and *Pseudomonas aeruginosa* using AFM. The sacculi were deposited on a flat silicon nitride surface with a series of parallel grooves (150 to 400 nm wide and 300 nm deep), and the AFM tip was forced onto the sacculus surface to deform it. They reported that the hydrated sacculi had an elastic modulus of  $2.5 \times 10^7$  N/m<sup>2</sup> while the dried sacculi with a higher value of modulus were more rigid and easily broken by AFM tip. Velegol et al. [124] also investigated the effects of cell elasticity to the shape of force curves. They found that the glutaraldehyde significantly affected the elasticity of the *E. coli* cells, but the nonlinear portion of the force curve and the nonlinear force were caused by the deformation of the bacterial surface layer. The same approach can be applied to measure the modulus of cellulose fibers and other macrobiomolecules [178, 179].



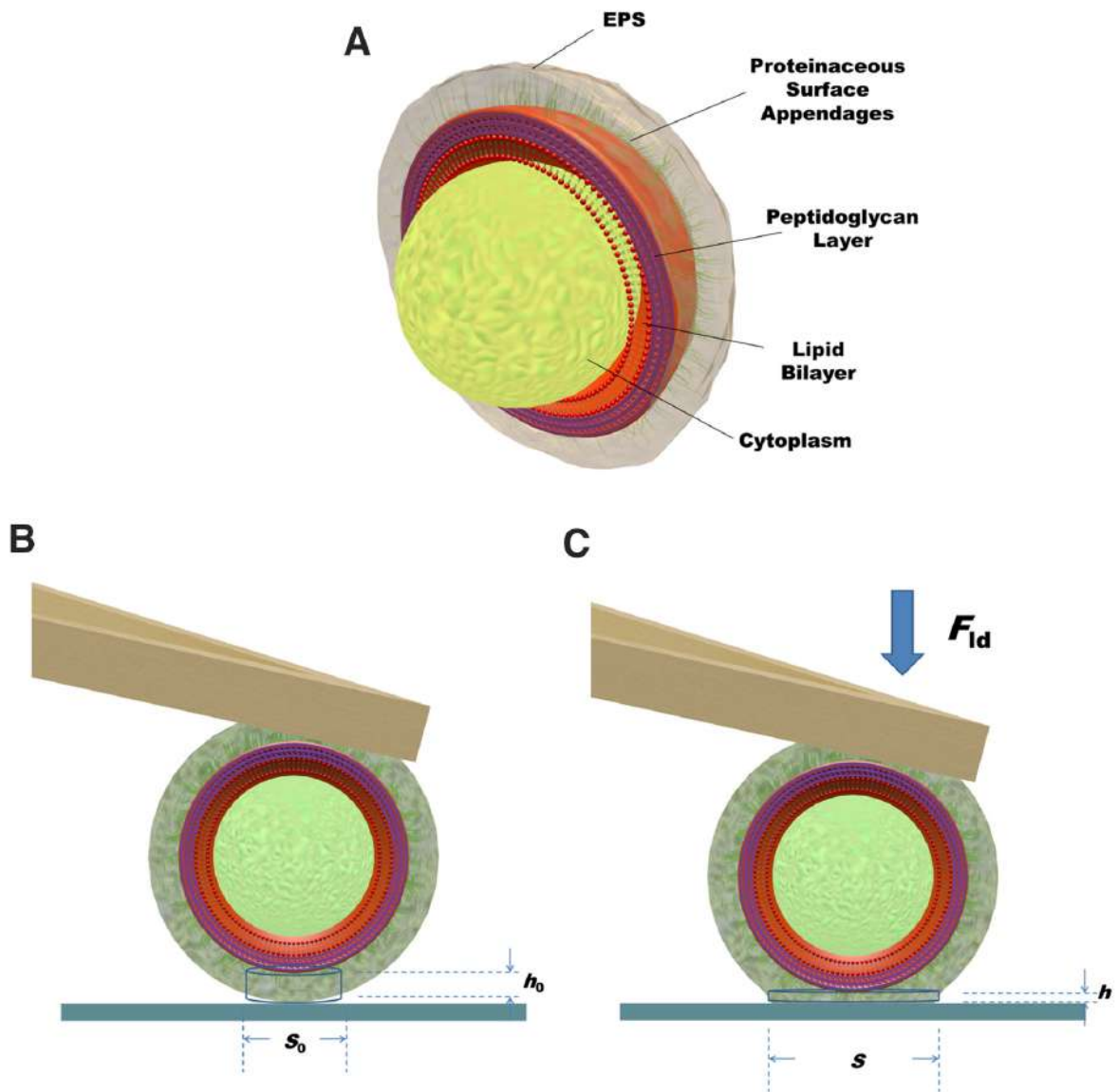


**Figure 8.** (A) Three-dimensional schematics showing the cell wall structure of a Gram-positive bacterial cell. (B) The initial contact between the cell and substrate surface without a loading force and any deformation. The contact volume is an imaginary cylinder with an initial area  $S_0$  and initial height  $h_0$ . (C) Upon the application of an external loading force the bacterial cell deforms and results in a cylinder with an area  $S$  and height  $h$  [180].

As the air bubble, bacterial cells are much softer compared to hard substrates or even the cantilever. The deformation of the cells during force measurement has a remarkable influence on the shape of force curve. Boulbitch [181] proposed a theoretical analysis for the deformation of the envelope of the Gram-negative bacteria caused by cantilever during the AFM measurements. They found that the rigidity of bacteria governed its turgor pressure whereas the lateral rigidity determined the distance from the tip where the displacement

vanished. Recently, Chen et al. [180] reported a method to determine the viscoelastic deformation of Gram-positive bacteria. As shown in Fig. 8, a spherical bacterium was attached to the end of a tipless cantilever, and the cell probe was pressed on a planar surface with a known extra loading force. The contact volume is represented by a cylinder with an initial area and initial height. They obtained the values of reduced Young's moduli ranging from 8 to 47 kPa by fitting the force-indentation curves to their modified model. Nanomechanical measurements can be carried out on the whole surface of a cell by force mapping [182]. Based on the single-cell force spectroscopy, Sullan and co-workers studied the nanospring properties of the pili during *Lactobacillus rhamnosus* GG-mucin interaction and calculated the spring constant of pilus ranging from 4.3 to 8.4 pN/nm [183].

#### 4. Theories for the interacting forces

Adhesion behavior of bacterial cells in aqueous environments is mediated by a sum of various physicochemical interactions, including the Lifshitz-Van der Waals forces, electrostatic interactions, steric forces, hydration and hydrophobic interactions. AFM force measurement data are often compared with quantitative theoretical models for a better understanding of physicochemical properties of microorganisms.

##### 4.1 Classical DLVO theory

Bacteria can be considered as colloidal particles because they are about 0.2-2  $\mu\text{m}$  in size. The classical DLVO theory was the first theory used to elucidate the interactions involved in bacterial adhesion. According to the classical DLVO theory, the total interaction forces between the particles consist of the attractive van der Waals force and the electrostatic double layer force, which can be either attractive or repulsive depending on the surface charge [184].

The van der Waals force was named after Johannes Diderik van der Waals to honor his contribution in the field of the equation of state for non-ideal gases. It is quantum mechanical in origin, and it arises from the time-dependent fluctuations in the electric dipole moment of a particle as it comes into contact with other particles nearby. The van der Waals forces are ever present, relatively long-range force, and not very sensitive to ionic strength of the solution. There are many different types of van der Waals' attractive forces, including London dispersive force, Debye inductive force and Keesom orientational force [126]. The van der Waals force between atoms and/or molecules is the sum of three different forces and

decays with the seventh power of the intermolecular distance [185]. Because the dispersion term dominates the van der Waals force, it is sometimes referred to as London dispersion forces [144].

The van der Waals interaction energy can be calculated using the Hamaker approach and/or the Lifshitz approach [185]. In the Hamaker approach for some simple geometries, all interaction energy splits into two terms, the Hamaker constant  $H = \pi^2 C \rho_1 \rho_2$  ( $\rho_i$  is the density of atoms or molecules) and another term that represents the geometrical dependence of the van der Waals energy [185]. Two commonly encountered geometries between macroscopic bodies include the interactions between two spheres or between a sphere and a flat surface. The calculation of van der Waals force for other geometries can be found in [126]. The van der Waals force between two spheres is given by:

$$F_{vdW} = -\frac{H}{6D^2} \frac{R_1 R_2}{R_1 + R_2} \quad (3)$$

where  $H$  is the Hamaker constant (J) which accounts for the interacting material properties and the third medium,  $D$  is the separation distance (m) between two interacting spheres,  $R_1$  or  $R_2$  is represents the radius of the spheres.

The van der Waals force between a sphere and a planar surface is given by:

$$F_{vdW} = -\frac{HR}{6D^2} \quad (4)$$

where  $R$  is the radius of the sphere.

Experimentally measured Hamaker constant between a variety of materials in different media is summarized in [126]. Typical values of the Hamaker constants are about  $10^{-20}$  to  $10^{-21}$  J in the case of biological cells or biomolecules interacting with themselves or minerals in aqueous environments [186]. The van der Waals force can be attractive or repulsive, but it is always attractive ( $H$  is positive) in the case of two identical particles immersed in a third aqueous medium.

As described above, the van der Waals interactions between identical particles are always attractive. However, in the colloidal suspension the aggregation does not always happen due

to the presence of a repulsive force. In the liquid of high dielectric constant, colloidal particles are usually charged on surfaces. Repulsion between identically charged particles is a long-range force, and is often sufficient to overcome the attractive effect of van der Waals force [187].

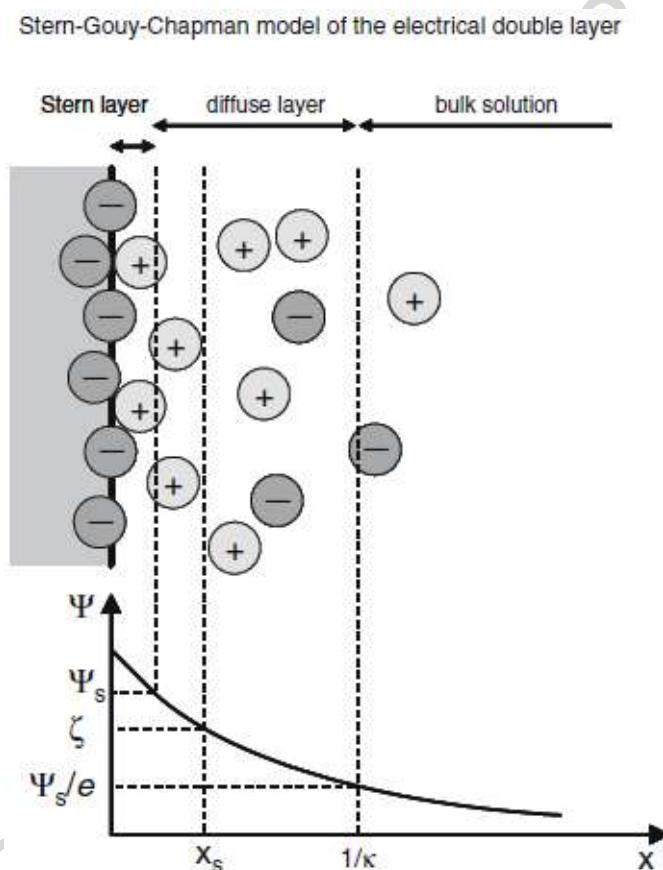


**Figure 9.** A schematic diagram showing the electrical double layer (EDL) on the surface of a particle, with the different potentials to be considered and the Debye length  $1/\kappa$  which is the length where the potential has fallen to a value of  $1/e$  of the Stern potential [188].

In water, many surfaces are charged. The charging of surfaces can come about in two mechanisms: 1) by the ionization or dissociation of surface groups (*e.g.* the dissociation of protons from carboxylic groups) which results in a charged surface; 2) by the adsorption of ions onto the previously uncharged surface (*e.g.* ion exchange) [187]. Since the whole system is electrically neutral, the overall charge on the particle surface is balanced by the dissolved counterions which carry opposite charge in the solution and diffuse uniformly throughout the bulk solution to increase the entropy [144]. As a result, a diffuse layer of counterions surrounding the charged surface is formed. Together, the diffuse layer and the charged surface immersed in an aqueous solution are called the electrical double layer (Fig. 9). When

two charged surfaces approach each other, their electrical double layer begin to overlap, resulting in a repulsive force if the surfaces are similarly charged.

The electrostatic double-layer forces can be calculated from the Poisson equation:

$$\nabla^2 \psi = -\frac{\rho}{\varepsilon_0 \varepsilon} \quad (5)$$

where  $\psi$  is the potential,  $\rho$  is the charge density at any position in between the approaching surfaces and  $\rho$  is given by:

$$\rho = \sum_{i=1}^N n_i z_i e \quad (6)$$

where  $n_i$  is the number density of the  $i^{\text{th}}$  ionic species,  $z_i$  is the valence of the  $i^{\text{th}}$  ionic species,  $e$  is the unit charge on electron.

The number density of the species can be given by Boltzmann equation:

$$n_i = n_{i\infty} \exp\left(-\frac{z_i e \psi}{k_B T}\right) \quad (7)$$

This equation (Equation (7)) is combined with Poisson equation (5) to give the following Poisson-Boltzmann equation:

$$\nabla^2 \psi = -\frac{e}{\varepsilon_0 \varepsilon} \sum_{i=1}^N z_i n_{i\infty} \exp\left(-\frac{z_i e \psi}{k_B T}\right) \quad (8)$$

Electrostatic double-layer forces are also very sensitive to the ionic strength and the composition of the liquid solution where the measurements are performed [15]. The thickness of the electrical double layer is represented by the ratio of the Coulombic potential to the thermal energy [185]. The so-called Debye constant  $\kappa$  is written in [185]:

$$\kappa = \sqrt{\frac{e^2 \sum n_i(\infty) z_i^2}{\varepsilon_0 \varepsilon k_B T}} \quad (9)$$

where  $e$  is the unit charge on electron,  $n_i(\infty)$  is the bulk concentration of the ion species  $i$  in ions per volume,  $z_i$  denotes the valence of ion species  $i$ ,  $\varepsilon$  is the relative permittivity of the solution ( $\varepsilon = 78.54$  at 298 K for water),  $\varepsilon_0$  is the permittivity of free space ( $8.854 \times 10^{-12} \text{ C}^2\text{J}^{-1}\text{m}^{-1}$ ),  $k_B$  is Boltzmann's constant,  $T$  is the absolute temperature, the summation is over all the electrolyte in the solution. The reciprocal of  $\kappa$  is the so-called Debye length which has unit of length.

When the surface potentials are smaller than about 50 mV, the interaction potential between a sphere ( $R$  is radius) and a planar surface at the separation of  $D$  can be mathematically described by [144]:

$$F_{EDL} = \frac{4\pi R\sigma_1\sigma_2}{\varepsilon_0\varepsilon\kappa} \times e^{-\kappa D} \quad (10)$$

The first approximate theory for the electrical double layer was given by Gouy, Chapman, Debye and Hückel. This theory assumes that the solvent is a structureless continuum, the ions are point charges and the potential of the mean force and the average electrostatic potential are the same [185]. In this theory the average charge and the corresponding electrical potential distribution are determined from the Poisson-Boltzmann equation, which is a second-order differential equation [126, 187]. To solve this equation two boundary conditions are often used:

- The surface potential remains constant (constant potential)
- The surface charge remains constant (constant charge)

Two surfaces with constant charge of equal sign always repel each other for  $D \rightarrow 0$ . Two surfaces with constant potential are attracted for  $D \rightarrow 0$  even when the surface potentials have the same sign (except for the hypothetical case that the potentials are precisely equal in magnitude and sign) [189].

The EDL force between two spheres or a sphere and a flat surface at constant surface potentials is described as:

$$F^\psi = \frac{2\pi\varepsilon_0\varepsilon\kappa R_x (2\psi_1\psi_2 e^{\kappa D} - \psi_1^2 - \psi_2^2)}{e^{2\kappa D} - 1} \quad (11)$$

where  $\psi_1$  and  $\psi_2$  are assumed to be the potentials of two interacting surfaces,  $R_x$  is equal to  $R_1R_2/(R_1 + R_2)$  ( $R_1$  and  $R_2$  represent the radius of two spheres and when one of them is a planar surface the radius is treated as infinite).

At the constant charge conditions, the EDL force is described as:

$$F^\sigma = \frac{2\pi\epsilon_0\epsilon\kappa R_x (2\psi_1\psi_2 e^{\kappa D} + \psi_{1\infty}^2 + \psi_{2\infty}^2)}{e^{2\kappa D} - 1} \quad (12)$$

where  $\psi_{1\infty}$  and  $\psi_{2\infty}$  are the potentials of two isolated bodies before interaction.

In addition to the above two cases, a third case has one surface at constant potential and the other at constant charge, which is important for the ionization or dissociation of amphoteric surfaces [185]. In the third case, the EDL force is given by:

$$F^{\sigma\psi} = \frac{2\pi\epsilon_0\epsilon\kappa R_x (2\psi_1\psi_{2\infty} e^{\kappa D} + \psi_1^2 - \psi_{2\infty}^2)}{e^{2\kappa D} + 1} \quad (13)$$

One should choose a more suitable boundary condition according to the interaction materials. In aqueous solutions, the DLVO theory can satisfactorily predict the interaction force for monovalent salts of dilute concentration and potentials below about 50 mV. However, due to the discontinuity of real surface charge distribution the prediction from DLVO theory for bivalent or trivalent ions leads to deviations [126].

Due to the dimensions, bacterial cells in the solution may be assumed to be colloidal particles. Accordingly, the DLVO theory has also been applied to describe the bacterial adhesion in a wide range of applications. A review was contributed by Hermansson [190]. However, many discrepancies between the experimental observations and the theoretical prediction have been reported. Rijnaarts et al. [191] reported that at low ionic strength the repulsive interactions predicted by the DLVO theory are orders of magnitude larger than experimentally obtained energy barriers. This difference is probably due to the attractive steric bridging effect. Camesano and Logan [13] studied the interactions between *Pseudomonas putida* KT2442 cells and silicon nitride cantilevers. They found that the range of measured repulsive forces is much larger than that predicted by DLVO theory. For more details regarding the comparison between experimental data and theoretic predictions, readers are referred to an excellent review of EDL interaction in bacterial adhesion [4]. In the DLVO theory, the interacting

surfaces are assumed to be perfectly smooth, with no asperities or surface structures. However, due to the complexity and heterogeneity of the structure and chemical components of microbial cells the prediction is not successful in many cases.

#### 4.2 Extended DLVO theory

Bacteria as well as other types of biological cells carry on their surface charged polymers that form a “soft” ion-penetrable layer around the cell [109]. Besides the DLVO forces, other forces such as Lewis acid base interactions, hydration forces and hydrophobic interactions may influence the bacterial adhesion process. To include these interaction forces between bacteria and the substrate, Van Oss [6] developed the extended DLVO model by considering the acid-base interactions which determine the hydrophobicity of the interaction surfaces:  $G^{total} = G^{vdW} + G^{EDL} + G^{AB}$ . A comparison between the DLVO and XDLVO predictions has been previously investigated by many researchers [184].

Similar to the DLVO theory, the extended DLVO model failed to describe bacterial adhesion process in many cases. This is probably attributed to the presence of cell surface polymers, which interfere with the DLVO-AB interactions. In 1998, Jucker et al. [192] developed a method to qualitatively infer the existence of polymer interactions between Gram-negative bacteria surface and glass, and quantify the interactions separately as the attractive or repulsive forces from the deviation of the adhesion from DLVO-AB based expectations. Their results indicate that the polymer interaction mainly govern the bacterial adhesion process.

Many other researchers employed the extended DLVO theory to calculate the interaction energies for bacterial adhesion. Roosjen and co-workers [193] assessed the energy of interaction between *Pseudomonas aeruginosa* strains and bare or brush-coated glass surface. They found that the attractive interaction between adhesive bacteria and the brush-coated glass is dominated by acid-base interactions according to the calculation from extended DLVO theory. Additionally, the calculated values for the interaction energy were in the same range as the adhesive energies derived from direct force measurements using AFM. The adhesion of *A. ferrooxidans* cells to pyrite and chalcopyrite surfaces was assessed using the extended DLVO theory [2]. They compared the values of Hamaker constant determined by microscopic and macroscopic methods and investigated the influence of Hamaker constant, ionic strength, interacting particle size and pH on the predicted interaction energy. They



found the macroscopic approach was more relevant. In summary, neither DLVO nor extended DLVO theories can fully interpret the bacterial adhesion behavior.

#### **4.3 Thermodynamic approach**

Surface thermodynamic approach is a macroscopic and physicochemical approach that interprets the role of hydrophobicity of bacteria and substrates surfaces by surface tension, but does not include an explicit role for electrostatic interactions. According to the thermodynamics, a system spontaneously undergoes a change to obtain a state of minimal energy [2].

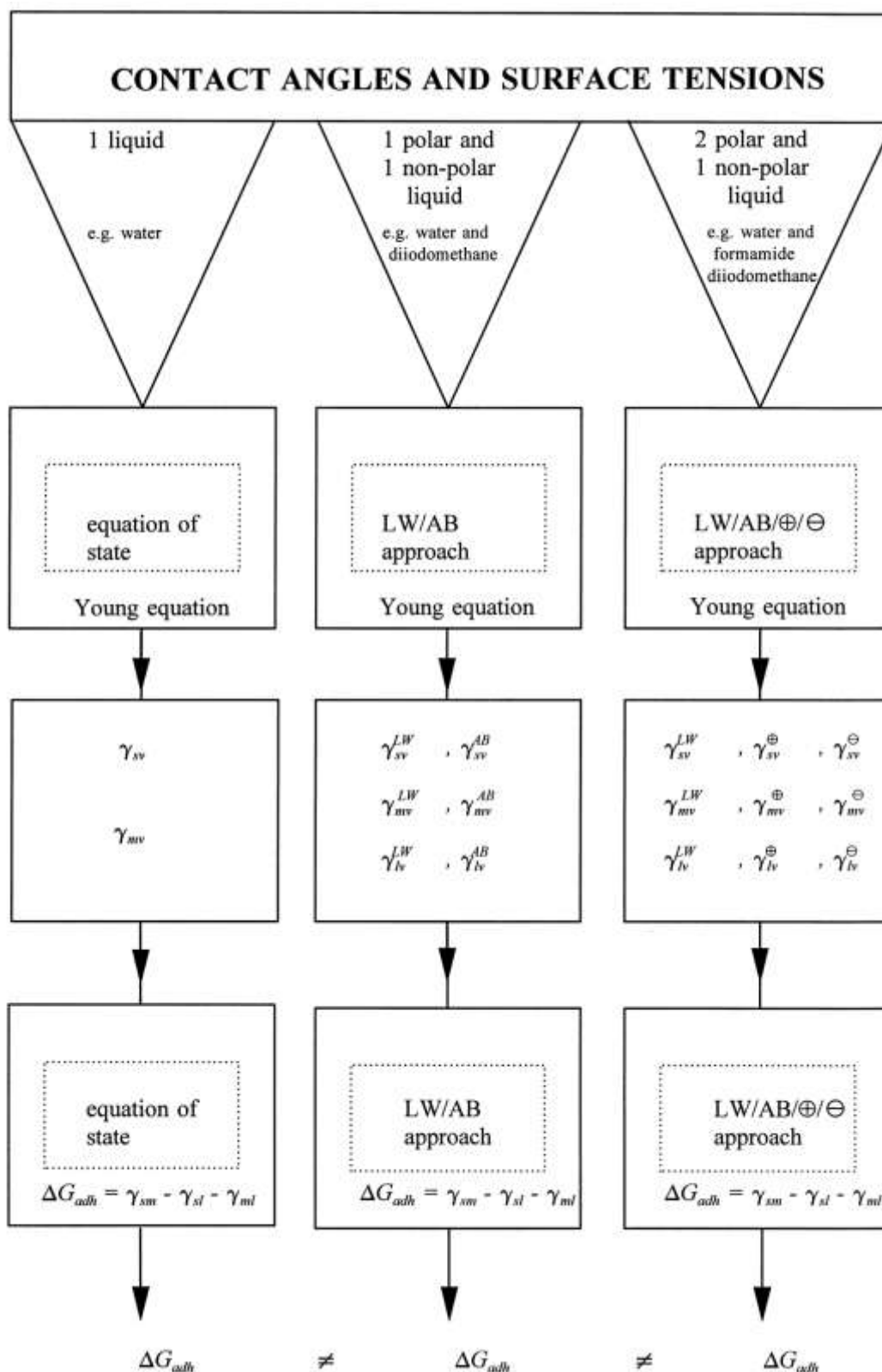


**Figure 10.** Theoretical estimation of the bacterial adhesion on solid surfaces by various thermodynamic approaches (Equation of state, Geometric mean approach and Lifshitz van der Waals acid/base approach) to convert contact angle data into surface free energy [116].

The thermodynamic approach is based on the free energy of the interacting surface, which is calculated as follows:

$$\Delta G_{adh} = \gamma_{sb} - (\gamma_{sl} + \gamma_{bl}) \quad (14)$$

where  $\gamma_{sb}$ ,  $\gamma_{sl}$  and  $\gamma_{bl}$  are the solid-bacteria, solid-liquid and bacteria-liquid interfacial free energies, respectively. In the case of bacteria-mineral interaction the adhesion of bacteria on the mineral surface leads to the formation of new interface, therefore the spontaneous attachment requires a decrease in free energy of the system, *i.e.*  $\gamma_{sb} < \gamma_{sl} + \gamma_{bl}$ . Similarly,  $\Delta G_{adh}$  in Eq. 14 can also be used to evaluate microbial co-adhesion by replacing the solid phase with a microbial cell [116].

In order to obtain value of  $\Delta G_{adh}$ , one should know the values of  $\gamma_{sb}$ ,  $\gamma_{sl}$  and  $\gamma_{bl}$ , which can be calculated from the measured contact angles of probe liquids with known or pre-characterized surface energy parameters (*e.g.* water, formamide and diiodomethane) on solid substrates and microbial lawns. To convert the contact angle into surface free energy, different approaches have been proposed, among which three major approaches frequently used are the equation of state approach, geometric mean approach and Lifshitz-van der Waals/acid-base approach (LW-AB) (Fig. 10) [116]. These theories are incompatible, and the value of  $\Delta G_{adh}$  differs depending on the approach used.

The thermodynamic approaches have been applied to the bioleaching system by different groups to interpret the adhesion behavior of bioleaching microorganisms. Gu et al. [194] reported that no adhesion between the *A. ferrooxidans* cells and the pyrite was obtained by the prediction of the thermodynamic approach, which is controversial to the experimental results. On the contrary, Vilinska et al. [2] found a good agreement between the thermodynamic prediction and the experimental results showing the adhesion of *A. ferrooxidans* on pyrite and chalcopyrite surface is energetically favourable. The microbial surface thermodynamics can be influenced by a variety of factors such the nutrient conditions, extracellular polymer production and cell surface structures. In addition, the thermodynamic approaches neglect the effect of electric charges and specific interactions (*e.g.* receptor-ligand), and assume that the adhesion process is reversible, which however is controversial

for the case of bacterial adhesion. Hence, the prediction of thermodynamic approach is generally inaccurate [195, 196].

#### 4.4 Steric model

On the approach of two surfaces covered by polymers, the thermally mobile polymer chains are confined from free movement at random. A decrease in entropy by confining these dangling chains causes a repulsive interaction, known as the steric or overlap repulsion [197]. This is similar to what occurs when a bacterial cell is approaching a substrate surface resulting in a narrowing interface. In general, the discrepancies between the experimental results and the theoretical calculation of DLVO/extended DLVO interactions are attributed to the interplay of bacterial surface biopolymers and the substrate surface.

Many biological cells have polymer-like surface components that contribute to the hydrophobicity including surface or S-layer proteins, amphipathic polymers or lipids. Cells-surface appendages (especially fimbriae) and possibly fibrillar glycoalyces (capsules) are considered as potential ‘probes’ bridging some bacterial cells to surfaces [68]. Due to the complicated spatial distribution of these macromolecular species, it is difficult to specify sharp boundaries where the forces overlap. However, steric repulsion does not necessarily have to be due to polymeric molecules. Layers of small molecules can have the same effect, albeit at a much shorter range [187]. The steric forces are often dominant the interactions between the bacteria and surfaces and can be modelled using a model developed for grafted polymer brush. The force per unit area between two interacting parallel flat surface, one of which is covered with polymer brush and one of which is bare, was modelled by Alexander [198] and de Gennes [199]. Drummond et al. [200] demonstrated that when the nominal radius of the tip is small enough they interact as spheres with radii between 100 and 400 nm. Based on this results, this model was later modified by Butt et al. [201] to describe the forces between a hemispherical AFM tip and a planar surface with polymer brush. By integrating the force per unit area over the AFM tip surface, the interaction force can be described as:

$$F_{st} = 50k_B T a L_0 \Gamma^{3/2} e^{-2\pi D/L_0} \quad (15)$$

where  $F_{st}$  is the total force due to steric interactions,  $a$  is the tip radius of curvature,  $L_0$  is the equilibrium polymer brush length,  $\Gamma$  is the grafted macromolecular density in the brush layer reflecting how much of the surface is covered by polymers,  $D$  is the separation distance.

The steric model has been applied to illustrate the AFM results involving AFM tip-cell interactions for bacteria such as *E. coli* [12, 202] and *Pseudomonas putida* [13, 203]. For the bioleaching microorganisms, Taylor et al. first [72] probed the thickness and grafting density of extracellular polymers on living *A. ferrooxidans* 23270 using an AFM tip cantilever in 0.1 M NaCl solution at pH 2. The results show that the calculated average polymer length is approximately 29 nm, and the polymer density is about  $7.1 \times 10^{16}$  molecules/m<sup>2</sup>. According to the length of biopolymers, they proposed that LPS is the dominant polymers on the outer surface of *A. ferrooxidans* grown with ferrous ion. Chandraprabha et al. [5] used the steric model to interpret the steric repulsion between a Si<sub>3</sub>N<sub>4</sub> AFM tip and an *A. ferrooxidans* cell under increasing pH and salt concentrations conditions. They found that  $L_0$  decreased from 176.7 nm at 0.001 M KCl solution to 8.5 nm at 1 M KCl solution. The polymer length at 0.1 M KCl solution is larger than that observed by Taylor et al. and is consistent with the electron microscopy result reported by Rojas [204]. They also found that after the removal of LPS on the cell surface, the resulting polymer length and grafting density dramatically decreased from 132.7 nm to 39.51 nm and from  $12.14 \times 10^{15}$  molecules/m<sup>2</sup> to  $7.45 \times 10^{15}$  molecules/m<sup>2</sup>, respectively.

Comparing the measured interaction forces to the theoretical models, DLVO and steric models, indicates that in high ionic strength and low pH solutions the steric force rather than the electrostatic force dominate the interactions between bacterial cells and the substrate surface.

## 5. Concluding remarks

This article has reviewed the diversity of bioleaching microorganism, cell surface properties, application of AFM in quantification of interaction forces and theoretical models relevant to the colloidal aspects for bioleaching microorganisms. As emphasized in this review, AFM is advantageous in operation under physiological conditions for the nanoscale microbe analysis by means of imaging and force measurements. A suitable model incorporating a variety of fundamental interaction forces should be optimal in interpretation of the bacteria-solid interactions. Technological challenges that remain to be addressed include the improvement of the protocols for firmly immobilizing a single living bioleaching cell to the AFM cantilever during the consecutive force measurements in various solution conditions.

## Acknowledgements

The authors gratefully acknowledge the University of Queensland postgraduate scholarship (UQRS).

## References

- [1] Schippers A, Hedrich S, Vasters J, Drobe M, Sand W, Willscher S, *Bio mining: Metal Recovery from Ores with Microorganisms*. Springer Berlin Heidelberg; 2013. p. 1-47.
- [2] Vilinska A, Hanumantha RK, *Open Colloid Sci J*, 2009; 2: 1-14.
- [3] Azeredo J, Visser J, Oliveira R, *Colloids Surf B Biointerface*, 1999; 14: 141-148.
- [4] Poortinga AT, Bos R, Norde W, Busscher HJ, *Surf Sci Rep*, 2002; 47: 1-32.
- [5] Chandraprabha MN, Somasundaran P, Natarajan KA, *Colloids Surf B Biointerface*, 2010; 75: 310-318.
- [6] van Oss CJ, *Colloids Surf A*, 1993; 78: 1-49.
- [7] Busscher HJ, Weerkamp AH, van der Mei HC, van Pelt AW, de Jong HP, Arends J, *Appl Environ Microb*, 1984; 48: 980-983.
- [8] Sharma PK, Hanumantha Rao K, *Colloids Surf B Biointerface*, 2003; 29: 21-38.
- [9] Dufrene YF, *J. Bacteriol.*, 2002; 184: 5205-5213.
- [10] Dorobantu LS, Gray MR, *Scanning*, 2010; 74-96.
- [11] Kuyukina MS, Korshunova IO, Rubtsova EV, Ivshina IB, *Appl Biochem Microbiol*, 2014; 50: 1-9.
- [12] Ong Y-L, Razatos A, Georgiou G, Sharma MM, *Langmuir*, 1999; 15: 2719-2725.
- [13] Camesano TA, Logan BE, *Environ Sci Technol*, 2000; 34: 3354-3362.
- [14] Farahat M, Hirajima T, Sasaki K, Doi K, *Colloids Surf B Biointerface*, 2009; 74: 140-149.
- [15] Dorobantu LS, Bhattacharjee S, Foght JM, Gray MR, *Langmuir*, 2009; 25: 6968-6976.
- [16] Farahat M, Hirajima T, Sasaki K, *J Colloid Interf Sci*, 2010; 349: 594-601.
- [17] Rawlings D, Dew D, du Plessis C, *Trends Biotechnol*, 2003; 21: 38 - 44.
- [18] Morin D, Lips A, Pinches T, Huisman J, Frias C, Norberg A, Forssberg E, *Hydrometallurgy*, 2006; 83: 69-76.

- [19] Zimmerley SR, Wilson DG, Prater JD, *Cyclic leaching process employing iron oxidizing bacteria*. 1958: US Patent 2. p. 829-964.
- [20] Colmer AR, Hinkle ME, *Science*, 1947; 106: 253-256.
- [21] Temple KL, Colmer AR, *J Bacteriol*, 1951; 62: 605-611.
- [22] Brierley C, Brierley J, *Appl Microbiol Biotechnol*, 2013; 97: 7543-7552.
- [23] Muñoz JA, Blázquez ML, Ballester A, González F, *Hydrometallurgy*, 1995; 38: 79-97.
- [24] Zhen S, Yan Z, Zhang Y, Wang J, Campbell M, Qin W, *Hydrometallurgy*, 2008; 96: 337-341.
- [25] Brierley JA, Brierley CL, *Hydrometallurgy*, 2001; 59: 233-239.
- [26] Olson GJ, Brierley JA, Brierley CL, *Appl Microbiol Biotechnol*, 2003; 63: 249-257.
- [27] Baker BJ, Banfield JF, *FEMS Microbiol Ecol*, 2003; 44: 139-152.
- [28] Schippers A, Microorganisms involved in bioleaching and nucleic acid-based molecular methods for their identification and quantification, in *Microbial Processing of Metal Sulfides*, Donati ER and Sand W, Editors., Springer; 2007. p. 3-33.
- [29] Donati ER, Sand W, SpringerLink: *Microbial Processing of Metal Sulfides*. 2007, Dordrecht: Springer Science+Business Media BV.
- [30] Hallberg KB, Johnson DB, *Adv Appl Microbiol*, 2001; 49: 37-84.
- [31] Dennison F, Sen AM, Hallberg KB, Johnson DB, Biological versus abiotic oxidation of iron in acid mine drainage waters: an important role for moderately acidophili, iron-oxidising bacteria, in *Biohydrometallurgy: Fundamentals, Technology and Sustainable Development*, Ciminelli VT and Garcia OJ, Editors., Elsevier Amsterdam; 2001. p. 493-501.
- [32] Johnson DB, Rolfe S, Hallberg KB, Iversen E, *Environ Microbiol*, 2001; 3: 630-637.
- [33] Pivovarova TA, Markosyan GE, Karavaiko GI, *Microbiology*, 1981; 50: 339-344.
- [34] Rawlings D, Coram N, Gardner M, Deane S, *Biohydrometallurgy and the environment toward the mining of the 21st century. Part A*, 1999; 777 - 786.
- [35] Hippe H, *Int J Sys Evol Microbiol*, 2000; 2: 501-503.
- [36] Ozkaya B, Sahinkaya E, Nurmi P, Kaksonen AH, Puhakka JA, *Hydrometallurgy*, 2007; 88: 67-74.
- [37] Johnson DB, Bacelar-Nicolau P, Okibe N, Thomas A, Hallberg KB, *Int J Syst Evol Microbiol*, 2009; 59: 1082-1089.

- [38] Golyshina O, Pivovarova T, Karavaiko G, Kondrat'eva T, Moore E, Abraham W, Lunsdorf H, Timmis K, Yakimov M, Golyshin P, *Int J Syst Evol Microbiol*, 2000; 50: 997 - 1006.
- [39] Lizama HM, Suzuki I, *Hydrometallurgy*, 1989; 22: 301-310.
- [40] Kamimura K, Higashino E, Kanao T, Sugio T, *Extremophiles*, 2005; 9: 45-51.
- [41] Hallberg KB, Lindström EB, *Microbiology*, 1994; 140: 3451 - 3456.
- [42] Dopson M, Lindström EB, *Appl Environ Microb*, 1999; 65: 36-40.
- [43] Moreira D, Amils R, *Int J Syst Bacteriol*, 1997; 47: 522-528.
- [44] Huber H, Stetter KO, *Arch Microbiol*, 1989; 151: 479-485.
- [45] Fuchs T, Huber H, Teiner K, Burggraf S, Stetter KO: *Metallosphaera prunae*, sp. nov., a novel metal-mobilizing, thermoacidophilic Archaeum, isolated from a uranium mine in Germany. Vol. 18. 1996, Jena, ALLEMAGNE: Elsevier.
- [46] Kurosawa N, Itoh YH, Itoh T, *Int J Syst Evol Microbiol*, 2003; 53: 1607-1608.
- [47] Kargi F, Robinson JM, *Biotechnol Bioeng*, 1985; 27: 41-49.
- [48] Vitaya VB, Koizumi J-I, Toda K, *J Ferment Bioeng*, 1994; 77: 528-534.
- [49] Silverman MP, Lundgren DG, *J Bacteriol*, 1959; 77: 642-647.
- [50] Kelly DP, Wood AP, *Int J Sys Evol Microbiol*, 2000; 50: 511-516.
- [51] Ishii M, Miyake T, Satoh T, Sugiyama H, Oshima Y, Kodama T, Igarashi Y, *Arch Microbiol*, 1996; 166: 368 - 71.
- [52] Huber G, Stetter KO, *Syst Appl Microbiol*, 1991; 14: 372-378.
- [53] Lobos JH, Chisolm TE, Bopp LH, Holmes DS, *Int J Syst Evo Bacteriol*, 1986; 36: 139-144.
- [54] Kusel K, Dorsch T, Acker G, Stackerbrandt E, *Appl Environ Microb*, 1999; 65: 3633-3640.
- [55] Clark DA, Norris PR, *Microbiology*, 1996; 142: 785 - 790.
- [56] Bogdanova TyI, Tsaplina IA, Kondrat'eva TF, Duda VI, Suzina NE, Melamud VS, Tourova TyP, Karavaiko GI, *Int J Syst Evol Microbiol*, 2006; 56: 1039-1042.
- [57] Norris PR, Clark DA, Owen JP, Waterhouse S, *Microbiology*, 1996; 142: 775-783.
- [58] McDonald IR, Kelly DP, Murrel JC, Wood AP, *Arch Microbiol*, 1997; 166: 394-398.
- [59] Rohwerder T, Gehrke T, Kinzler K, Sand W, *Appl Microbiol Biotechnol*, 2003; 63: 239-248.



- [60] Edwards KJ, Goebel BM, Rodgers TM, Schrenk MO, Gihring TM, Cardona MM, Hu B, McGuire MM, Hamers RJ, Pace NR, Banfield JF, *Geomicrobiol J*, 1999; 16: 155-179.
- [61] Bond PL, Smriga SP, Banfield JF, *Appl Environ Microb*, 2000; 66: 3842-3849.
- [62] Kelly DP, Harrison AH, Genus *Thiobacillus*, in *Bergey's Manual of Systematic Bacteriology*, 1st edn, Staley JT, et al., Editors., Williams & Wilkins Baltimore; 1989. p. 1842-1858.
- [63] Johnson DB, *FEMS Microbiol Ecol*, 1998; 27: 307 - 317.
- [64] Mozes N: *Microbial cell surface analysis: structural and physicochemical methods*. 1991, New York: VCH Publishers.
- [65] Hammond SM, Rycroft AN, Lambert PA: *The bacterial cell surface*. 1984, London: Kapitan Szabo Publishers.
- [66] Hancock I, Poxton I: *Bacterial cell surface techniques*. 1988, Chichester [West Sussex] ; New York: Wiley.
- [67] Walker SL, Redman JA, Elimelech M, *Langmuir*, 2004; 20: 7736-7746.
- [68] Skvarla J, *J Chem Soc, Faraday Trans*, 1993; 89: 2913-2921.
- [69] Burks GA, Velegol SB, Paramonova E, Lindenmuth BE, Feick JD, Logan BE, *Langmuir*, 2003; 19: 2366-2371.
- [70] Escobar B, Huerta G, Rubio J, *World Journal of Microbiology and Biotechnology*, 1997; 13: 593-594.
- [71] Chandraprabha MN, Natarajan KA, *Int J Miner Process*, 2013; 123: 152-157.
- [72] Taylor ES, Lower SK, *Appl Environ Microb*, 2008; 74: 309-311.
- [73] Ohmura N, Tsugita K, Koizumi J, Saika H, *J. Bacteriol.*, 1996; 178: 5776-5780.
- [74] Li Y-Q, Wan D-S, Huang S-S, Leng F-F, Yan L, Ni Y-Q, Li H-Y, *Curr Microbiol*, 2010; 60: 17-24.
- [75] Korhonen TK, Nurmiäho E-L, Tuovinen OH, *FEMS Microbiology Letters*, 1978; 3: 195-198.
- [76] Liu J-s, Xie X-h, Xiao S-m, Wang X-m, Zhao W-j, Tian Z-l, *J Cent South Univ Technol*, 2007; 14: 467-473.
- [77] Sand W, Rohde K, Sobotke B, Zenneck C, *Appl Environ Microb*, 1992; 58: 85-92.
- [78] Doetsch RN, Cook TM, Vaituzis Z, *Antonie van Leeuwenhoek*, 1967; 33: 196-202.
- [79] Waksman SA, Joffe JS, *J Bacteriol*, 1922; 7: 239-256.

- [80] Characklis WG, Wilderer PA: Structure and function of biofilms: report of the Dahlem Workshop on Structure and Function of Biofilms, Berlin, 1988, November 27-December 2. Vol. 46. 1989, Chichester, England ; New York: Wiley.
- [81] Wingender J, Flemming H-C, Neu TR: Microbial extracellular polymeric substances: characterization, structure, and function. 1999, New York: Springer.
- [82] Sand W, Gehrke T, Res Microbiol, 2006; 157: 49-56.
- [83] Zhu J, Li Q, Jiao W, Jiang H, Sand W, Xia J, Liu X, Qin W, Qiu G, Hu Y, Chai L, Coloids Surf B Biointerface, 2012; 94: 95-100.
- [84] Vilinska A, Rao KH, Miner Metall Process, 2011; 28: 151-158.
- [85] Devasia P, Natarajan KA, Sathyanarayana DN, Rao GR, Appl Environ Microb, 1993; 59: 4051-4055.
- [86] Sharma PK, Das A, Hanumantha Rao K, Forssberg KSE, Hydrometallurgy, 2003; 71: 285-292.
- [87] Blake RC, II, Shute EA, Howard GT, Appl Environ Microb, 1994; 60: 3349-3357.
- [88] Diao M, Taran E, Mahler S, Nguyen TAH, Nguyen AV, Coloids Surf B Biointerface, 2014; 115: 229-236.
- [89] Florian B, Noël N, Thyssen C, Felschau I, Sand W, Miner Eng, 2011; 24: 1132-1138.
- [90] Brown MJ, Lester JN, Appl Environ Microb, 1980; 40: 179-185.
- [91] Azeredo J, Lazarova V, Oliveira R, Water Sci Technol, 1999; 39: 243-250.
- [92] McCourtie J, Douglas LJ, J Gen Microbiol, 1985; 131: 495-503.
- [93] Liu H, Fang HHP, Journal of Biotechnology, 2002; 95: 249-256.
- [94] Sheng G-P, Yu H-Q, Yu Z, Appl Microbiol Biotechnol, 2005; 67: 125-130.
- [95] Sheng G-P, Yu H-Q, Li X-Y, Biotechnol Adv, 2010; 28: 882-894.
- [96] Gehrke T, Telegdi J, Thierry D, Sand W, Appl Environ Microb, 1998; 64: 2743 - 2747.
- [97] Zeng W, Qiu G, Zhou H, Liu X, Chen M, Chao W, Zhang C, Peng J, Hydrometallurgy, 2010; 100: 177-180.
- [98] Xia L, Shen Z, Vargas T, Sun W, Ruan R, Xie Z, Qiu G, Biotechnol Lett, 2013; 1-8.
- [99] Geoghegan M, Andrews JS, Biggs CA, Eboigbodin KE, Elliott DR, Rolfe S, Scholes J, Ojeda JJ, Romero-Gonzalez ME, Edyvean RGJ, Swanson L, Rutkaite R, Fernando R, Pen Y, Zhang Z, Banwart SA, Faraday Discuss, 2008; 139: 85-103.
- [100] Sharma PK, Hanumantha Rao K, Adv Colloid Interface Sci, 2002; 98: 341-463.

- [101] Gallardo-Moreno AM, Navarro-Pérez ML, Vadillo-Rodríguez V, Bruque JM, González-Martín ML, *Coloids Surf B Biointerface*, 2011; 88: 373-380.
- [102] van der Mei HC, Bos R, Busscher HJ, *Coloids Surf B Biointerface*, 1998; 11: 213-221.
- [103] Vilinska A, Rao KH, *Geomicrobiol J*, 2011; 28: 221-228.
- [104] Bellon-Fontaine MN, Rault J, van Oss CJ, *Coloids Surf B Biointerface*, 1996; 7: 47-53.
- [105] Rosenberg M, Gutnick D, Rosenberg E, *FEMS Microbiology Letters*, 1980; 9: 29-33.
- [106] Skvarla J, Kupka D, Turcaniova L, *Acta Montan Slovaca*, 1998; 3: 368-377.
- [107] Gu G, Su L, Chen M, Sun X, Zhou H, *Min Sci Technol (Xuzhou, China)*, 2010; 20: 286-291.
- [108] Devasia P, Natarajan KA, *Int J Miner Process*, 2010; 94: 135-139.
- [109] Ohshima H, Kondo T, *Biophys Chem*, 1991; 39: 191-198.
- [110] Dittrich M, Sibling S, *J Colloid Interf Sci*, 2005; 286: 487-495.
- [111] Asami K, *J Non-Cryst Solids*, 2002; 305: 268-277.
- [112] Bowen WR, Lovitt RW, Wright CJ, *Colloids Surf A*, 2000; 173: 205-210.
- [113] Bowen WR, Fenton AS, Lovitt RW, Wright CJ, *Biotechnol Bioeng*, 2002; 79: 170-179.
- [114] Sheng X, Ting YP, Pehkonen SO, *J Colloid Interf Sci*, 2008; 321: 256-264.
- [115] van Loosdrecht MC, Lyklema J, Norde W, Zehnder AJ, *Microbiol Mol Biol Rev*, 1990; 54: 75-87.
- [116] Bos R, van der Mei HC, Busscher HJ, *FEMS Microbiol Rev*, 1999; 23: 179-230.
- [117] Watling HR, *Hydrometallurgy*, 2006; 84: 81-108.
- [118] Edwards KJ, Hu B, Hamers RJ, Banfield JF, *FEMS Microbiol Ecol*, 2001; 34: 197-206.
- [119] Gautier V, Escobar B, Vargas T, *Hydrometallurgy*, 2008; 94: 121-126.
- [120] Sanhueza A, Ferrer IJ, Vargas T, Amils R, Sánchez C, *Hydrometallurgy*, 1999; 51: 115-129.
- [121] Taubenberger AV, Hutmacher DW, Muller DJ, *Tissue Eng, Part B*, 2014; 20: 40-55.
- [122] Binnig G, Quate CF, Gerber C, *Phys Rev Lett*, 1986; 56: 930.

- [123] Beaussart A, El-Kirat-Chatel S, Herman P, Alsteens D, Mahillon J, Hols P, Dufrêne Yves F, *Biophys J*, 2013; 104: 1886-1892.
- [124] Velegol SB, Logan BE, *Langmuir*, 2002; 18: 5256-5262.
- [125] Watson GS, Blach JA, Cahill C, Nicolau DV, Pham DK, Wright J, Myhra S, *Biosens Bioelectron*, 2004; 19: 1355-1362.
- [126] Butt H-J, Cappella B, Kappl M, *Surf Sci Rep*, 2005; 59: 1-152.
- [127] Butt H-J, *Biophys J*, 1991; 60: 1438-1444.
- [128] Ducker WA, Senden TJ, Pashley RM, *Nature*, 1991; 353: 239-241.
- [129] Dorobantu LS, Bhattacharjee S, Foght JM, Gray MR, *Langmuir*, 2008; 24: 4944-4951.
- [130] Heinz WF, Hoh JH, *Trends Biotechnol*, 1999; 17: 143-150.
- [131] Weisenhorn AL, Maivald P, Butt HJ, Hansma PK, *Phys Rev B*, 1992; 45: 11226.
- [132] Louise Meyer R, Zhou X, Tang L, Arpanaei A, Kingshott P, Besenbacher F, *Ultramicroscopy*, 2010; 110: 1349-1357.
- [133] Kasas S, Ikai A, *Biophys J*, 1995; 68: 1678-1680.
- [134] Gad M, Ikai A, *Biophys J*, 1995; 69: 2226-2233.
- [135] Ubbink J, Schär-Zammaretti P, *Micron*, 2005; 36: 293-320.
- [136] Doktycz MJ, Sullivan CJ, Hoyt PR, Pelletier DA, Wu S, Allison DP, *Ultramicroscopy*, 97: 209-216.
- [137] Lower SK, Tadanier CJ, Hochella Jr MF, *Geochim Cosmochim Acta*, 2000; 64: 3133-3139.
- [138] Yao X, Walter J, Burke S, Stewart S, Jericho MH, Pink D, Hunter R, Beveridge TJ, *Colloids Surf B Biointerface*, 2002; 23: 213-230.
- [139] Bowen WR, Hilal N, Lovitt RW, Wright CJ, *Colloids Surf A*, 1998; 136: 231-234.
- [140] Kang S, Elimelech M, *Langmuir*, 2009; 25: 9656-9659.
- [141] Razatos A, Ong Y-L, Sharma MM, Georgiou G, *Proceedings of the National Academy of Sciences of the United States of America*, 1998; 95: 11059-11064.
- [142] Sheng X, Ting YP, Pehkonen SO, *J Colloid Interf Sci*, 2007; 310: 661-669.
- [143] Cao T, Tang H, Liang X, Wang A, Auner GW, Salley SO, Ng KYS, *Biotechnol Bioeng*, 2006; 94: 167-176.
- [144] Butt H-J, Jaschke M, Ducker W, *Bioelectrochem Bioenerg*, 1995; 38: 191-201.

- [145] Gunning AP, Kirby AR, Morris VJ, Wells B, Brooker BE, *Polymer Bulletin*, 1995; 34: 615-619.
- [146] Bremer PJ, Geese GG, Drake B, *Curr Microbiol*, 1992; 24: 223-230.
- [147] Steele A, Goddard DT, Beech IB, *Int Biodeterior Biodegrad*, 1994; 34: 35-46.
- [148] Mangold S, Laxander M, Harneit K, Rohwerder T, Claus G, Sand W, *Hydrometallurgy*, 2008; 94: 127-132.
- [149] Noël N, Florian B, Sand W, *Hydrometallurgy*, 2010; 104: 370-375.
- [150] Francius G, Polyakov P, Merlin J, Abe Y, Ghigo J-M, Merlin C, Beloin C, Duval JFL, *PLoS ONE*, 2011; 6: e20066.
- [151] Lyubchenko Y, Shlyakhtenko L, Harrington R, Oden P, Lindsay S, *Proceedings of the National Academy of Sciences*, 1993; 90: 2137-2140.
- [152] Hansma HG, Laney DE, Bezanilla M, Sinsheimer RL, Hansma PK, *Biophys J*, 1995; 68: 1672-1677.
- [153] Gunning AP, Morris VJ, Kirby AR: *Atomic force microscopy for biologists*. 1999, London: Imperial College Press.
- [154] Dupres V, Verbelen C, Dufrêne YF, *Biomaterials*, 2007; 28: 2393-2402.
- [155] Yang J, Mou J, Shao Z, *Febs Lett*, 1994; 338: 89-92.
- [156] Abu-Lail NI, Camesano TA, *J Microsc*, 2003; 212: 217-238.
- [157] Bevilaqua D, Diéz-Perez I, Fugivara CS, Sanz F, Benedetti AV, Garcia O, *Bioelectrochemistry*, 2004; 64: 79-84.
- [158] Florian B, Noël N, Sand W, *Miner Eng*, 2010; 23: 532-535.
- [159] Becker T, Gorham N, Shiers DW, Watling HR, *Process Biochem*, 2011; 46: 966-976.
- [160] van der Aa BC, Dufrêne YF, *Coloids Surf B Biointerface*, 2002; 23: 173-182.
- [161] González D, Lara R, Alvarado K, Valdez-Pérez D, Navarro-Contreras H, Cruz R, García-Meza J, *Appl Microbiol Biotechnol*, 2011; 1-13.
- [162] Emerson RJ, Camesano TA, *Appl Environ Microb*, 2004; 70: 6012-6022.
- [163] Lower SK, *Am J Sci*, 2005; 305: 752-765.
- [164] Dufrêne YF, *Micron*, 2001; 32: 153-165.
- [165] Dufrêne FY, Hinterdorfer P, *Pflügers Archiv - European Journal of Physiology*, 2007; 456: 237-245.
- [166] Dufrêne YF, *mBio*, 2014; 5.

- [167] Grantham MC, Dove PM, *Geochim Cosmochim Acta*, 1996; 60: 2473-2480.
- [168] Fang HHP, Chan K-Y, Xu L-C, *J Microbiol Methods*, 2000; 40: 89-97.
- [169] Lara RH, Valdez-Pérez D, Rodríguez AG, Navarro-Contreras HR, Cruz R, García-Meza JV, *Hydrometallurgy*, 2010; 103: 35-44.
- [170] Diao M, Nguyen TAH, Taran E, Mahler S, Nguyen AV, *Miner Eng*, 2014; 61: 9-15.
- [171] Zhang W, Stack AG, Chen Y, *Colloids Surf B Biointerface*, 2011; 82: 316-324.
- [172] Xu H, Murdaugh AE, Chen W, Aidala KE, Ferguson MA, Spain EM, Núñez ME, *Langmuir*, 2013; 29: 3000-3011.
- [173] Lau PCY, Dutcher JR, Beveridge TJ, Lam JS, *Biophys J*, 2009; 96: 2935-2948.
- [174] Wang H, Wilksch JJ, Lithgow T, Strugnell R, Gee ML, *Soft Matter*, 2013; 9: 7560-7567.
- [175] van der Mei HC, Busscher HJ, Bos R, de Vries J, Boonaert CJP, Dufrêne YF, *Biophys J*, 2000; 78: 2668-2674.
- [176] Alsteens D, Van Dijck P, Lipke PN, Dufrêne YF, *Langmuir*, 2013.
- [177] Yao X, Jericho M, Pink D, Beveridge T, *J Bacteriol*, 1999; 181: 6865-6875.
- [178] Guhados G, Wan W, Hutter JL, *Langmuir*, 2005; 21: 6642-6646.
- [179] Rief M, Oesterhelt F, Heymann B, Gaub HE, *Science*, 1997; 275: 1295-1297.
- [180] Chen Y, Norde W, van der Mei HC, Busscher HJ, *mBio*, 2012; 3.
- [181] Boulbitch A, *J Electron Microsc*, 2000; 49: 459-462.
- [182] Longo G, Rio LM, Trampuz A, Dietler G, Bizzini A, Kasas S, *J. Microbiol. Methods*, 2013; 93: 80-84.
- [183] Sullan RMA, Beaussart A, Tripathi P, Derclaye S, El-Kirat-Chatel S, Li JK, Schneider Y-J, Vanderleyden J, Lebeer S, Dufrene YF, *Nanoscale*, 2014.
- [184] Bayouhd S, Othmane A, Mora L, Ben Ouada H, *Colloids Surf B Biointerface*, 2009; 73: 1-9.
- [185] Nguyen AV, Schulze HJ: *Colloidal science of flotation*. Vol. 118. 2004, New York: Marcel Dekker.
- [186] Kendall TA, Lower SK, *Forces between Minerals and Biological Surfaces in Aqueous Solution*, in *Adv Agron*. Academic Press; 2004. p. 1-54.
- [187] Bowen WR, Hilal N: *Atomic force microscopy in process engineering: introduction to AFM for improved processes and products*. 2009, Burlington, Mass: Butterworth Heinemann.

- [188] Handy R, von der Kammer F, Lead J, Hassellöv M, Owen R, Crane M, *Ecotoxicology*, 2008; 17: 287-314.
- [189] Barouch E, Matijevic E, *J Chem Soc, Faraday Trans. 1*, 1985; 81: 1797-1817.
- [190] Hermansson M, *Coloids Surf B Biointerface*, 1999; 14: 105-119.
- [191] Rijnaarts HHM, Norde W, Lyklema J, Zehnder AJB, *Coloids Surf B Biointerface*, 1999; 14: 179-195.
- [192] Jucker BA, Zehnder AJB, Harms H, *Environ Sci Technol*, 1998; 32: 2909-2915.
- [193] Roosjen A, Busscher HJ, Norde W, van der Mei HC, *Microbiology*, 2006; 152: 2673-2682.
- [194] Gu G, Wang H, Suo J, Qiu G, Hao Y, *J Cent South Univ Technol*, 2008; 15: 49-53.
- [195] Strevett KA, Chen G, *Res Microbiol*, 2003; 154: 329-335.
- [196] Katsikogianni M, Missirlis YF, *Eur Cells Mater*, 2004; 8: 37-57.
- [197] Israelachvili JN: *Intermolecular and surface forces*. 1992, London ; New York: Academic Press.
- [198] Alexandra S, *J Phys*, 1977; 38: 983-987.
- [199] de Gennes PG, *Adv Colloid Interface Sci*, 1987; 27: 189-209.
- [200] Drummond CJ, Senden TJ, *Colloids Surf A*, 1994; 87: 217-234.
- [201] Butt H-J, Kappl M, Mueller H, Raiteri R, Meyer W, Rühle J, *Langmuir*, 1999; 15: 2559-2565.
- [202] Abu-Lail NI, Camesano TA, *Environ Sci Technol*, 2003; 37: 2173-2183.
- [203] Abu-Lail NI, Camesano TA, *Biomacromolecules*, 2003; 4: 1000-1012.
- [204] Rojas J, Giersig M, Tributsch H, *Arch Microbiol*, 1995; 163: 352-356.

**Figure captions**

**Figure 1.** Schematic of the cell wall structure of Gram-negative bacteria with several surface appendages

**Figure 2.** Schematic of bacteria-mineral interactions in a bioleaching system

**Figure 3.** Schematic of an atomic force microscope and a force measurement cycle

**Figure 4.** (a) Schematic of the biological force microscopy showing one of many possible poly-lysine linkages between negatively charged silanol groups on the bead and negatively charged cell-surface functional groups on biomolecules. (b) Scanning laser confocal micrograph of a biologically-active-force-probe (BAFP) . Scale bar 10  $\mu\text{m}$

**Figure 5.** Bacterial morphology observed by the contact mode of AFM in air. AFM height and deflection images of four strains of *E. coli* (a. E2152; b. E2146; c. E2302 and d. E2498) acquired in air shown in height and deflection images with a z-scale of 200 nm

**Figure 6.** AFM and epifluorescence microscope (EFM) image of *A. ferrooxidans* cells attached to pyrite. A: Vertical deflection image obtained by contact mode in air. B: Vertical deflection image acquired with tapping mode in mineral salt solution. C: EFM image of the same sample location

**Figure 7.** Force spectroscopy of cell-cell interaction using wedged cantilevers. (a) SEM image of a wedged cantilever. (b) A cell probe (labeled with green Con A-FITC) prepared from a nondestructive method approached a *C. albicans* hyphae (Calcofluor White, blue) which was immobilized on a hydrophobic substrate. The yeast cell probe was positioned on top of the yeast region (c, e) or the germ tube region of the hyphae (d, f) with the corresponding representative force-distance curves (e, f)

**Figure 8.** (A) Three-dimensional schematics showing the cell wall structure of a Gram-positive bacterial cell. (B) The initial contact between the cell and substrate surface without a loading force and any deformation. The contact volume is an imagery cylinder with an initial area and initial height. (C) Upon the application of an external loading force the bacterial cell deforms and results in a cylinder with a large area and height

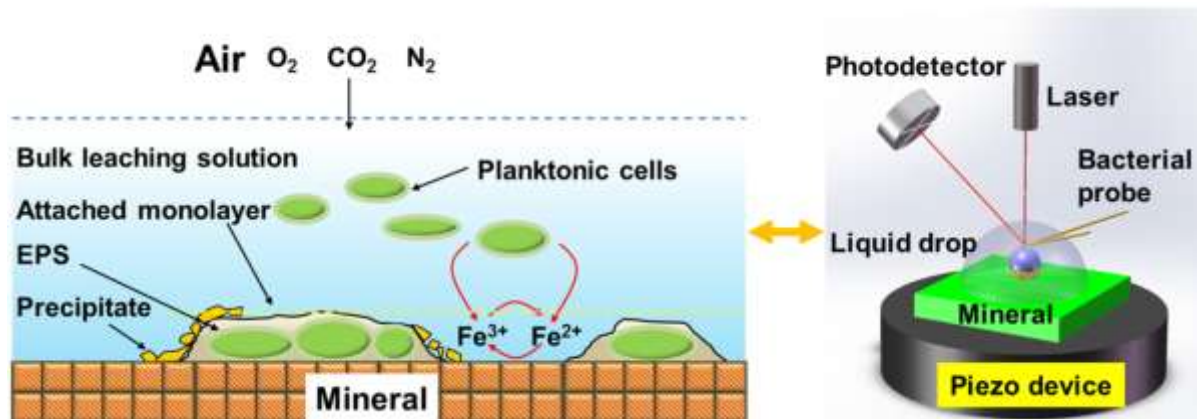


**Figure 9.** A schematic diagram showing the electrical double layer (EDL) on the surface of a particle, with the different potentials to be considered and the Debye length which is the length where the potential has fallen to a value of the Stern potential.

**Figure 10.** Theoretical estimation of the bacterial adhesion on solid surfaces by various thermodynamic approaches (Equation of state, Geometric mean approach and Lifshitz van der Waals acid/base approach) to convert contact angle data into surface free energy

ACCEPTED MANUSCRIPT

## Graphical abstract



**Highlights:**

- Bacteria adhesion to mineral surfaces mediates bioleaching processes.
- Bacterial surface appendages and EPS play a vital role in adhesion.
- Review of quantitative measurements of bacteria-solid interaction forces using AFM.
- DLVO and thermodynamic theories cannot fully explain bacterial adhesion behaviour.
- Steric forces dominate the interaction between cells and substrate surfaces.